



*The Abdus Salam*  
**International Centre for Theoretical Physics**



**2256-18**

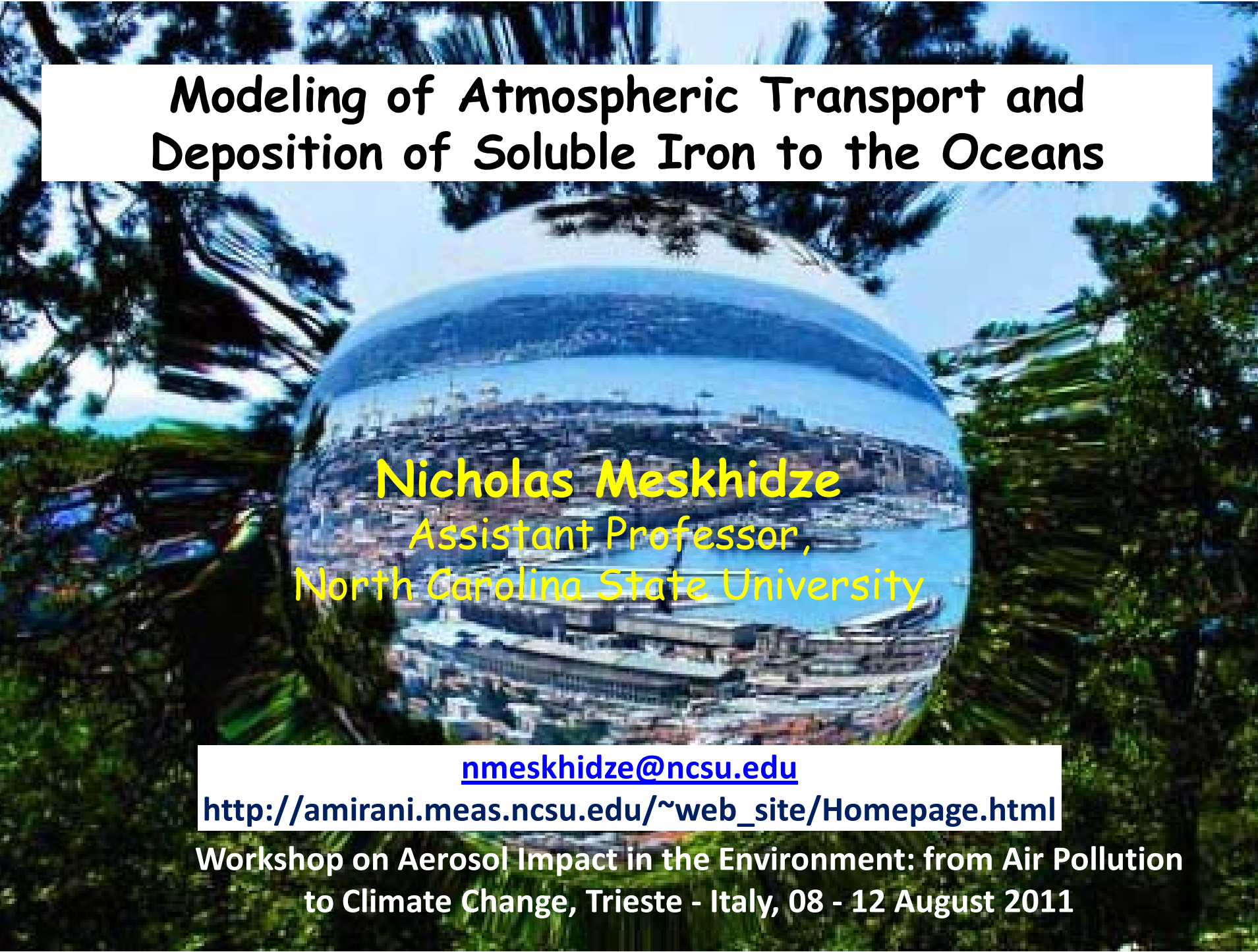
**Workshop on Aerosol Impact in the Environment: from Air Pollution to  
Climate Change**

*8 - 12 August 2011*

**Modeling of Atmospheric Transport and Deposition of Soluble Iron to the Oceans**

N. Meskhidze

*North Caroline State Univ., Raleigh  
USA*



# Modeling of Atmospheric Transport and Deposition of Soluble Iron to the Oceans

Nicholas Meskhidze  
Assistant Professor,  
North Carolina State University

[nmeskhidze@ncsu.edu](mailto:nmeskhidze@ncsu.edu)

[http://amirani.meas.ncsu.edu/~web\\_site/Homepage.html](http://amirani.meas.ncsu.edu/~web_site/Homepage.html)

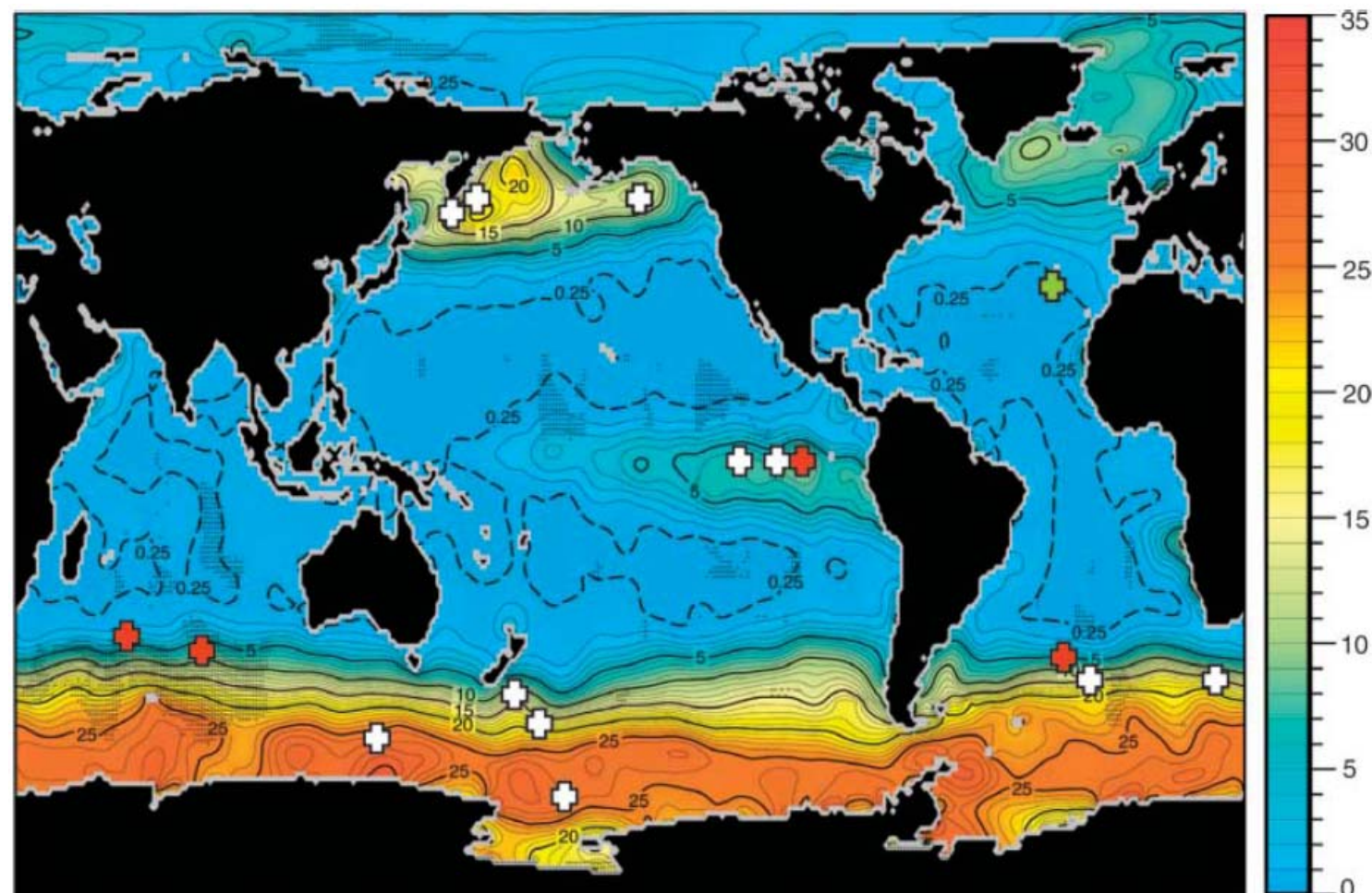
Workshop on Aerosol Impact in the Environment: from Air Pollution  
to Climate Change, Trieste - Italy, 08 - 12 August 2011

# Overview



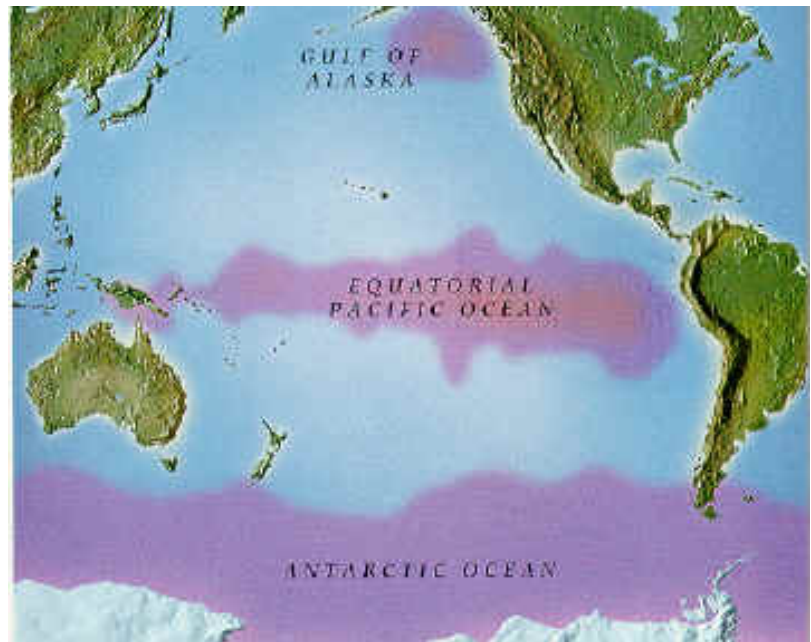
- 1) Introduction & motivation
- 2) Acid dissolution of iron in mineral dust aerosols
- 3) Lagrangian equilibrium model
- 4) Other mechanisms for iron dissolution
- 5) Case studies using GEOS-Chem/DFeS

## Background: High Nitrate Low Chlorophyll (HNLC) Waters

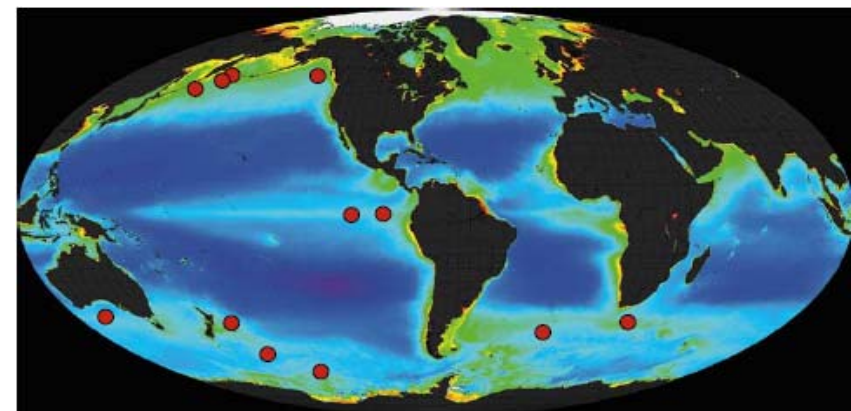
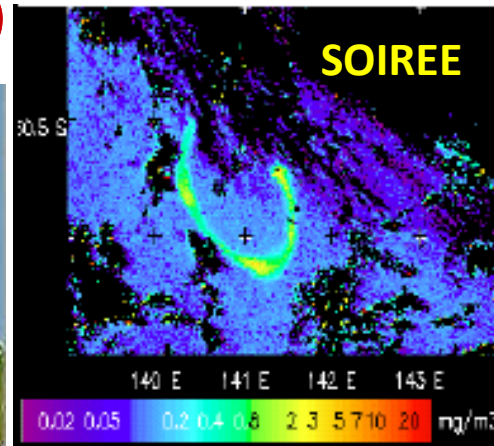


[Source: Boyd, et al. *Science*, 2007 ]

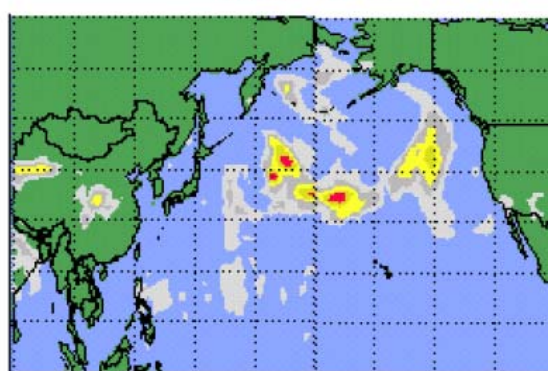
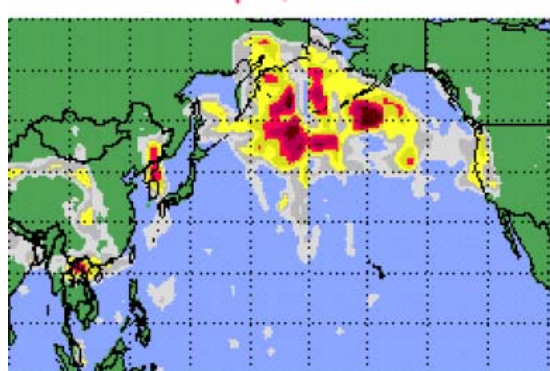
## Background (continued)



High-nitrate low-chlorophyll (HNLC) regions  
Largest inventories of unused nutrients

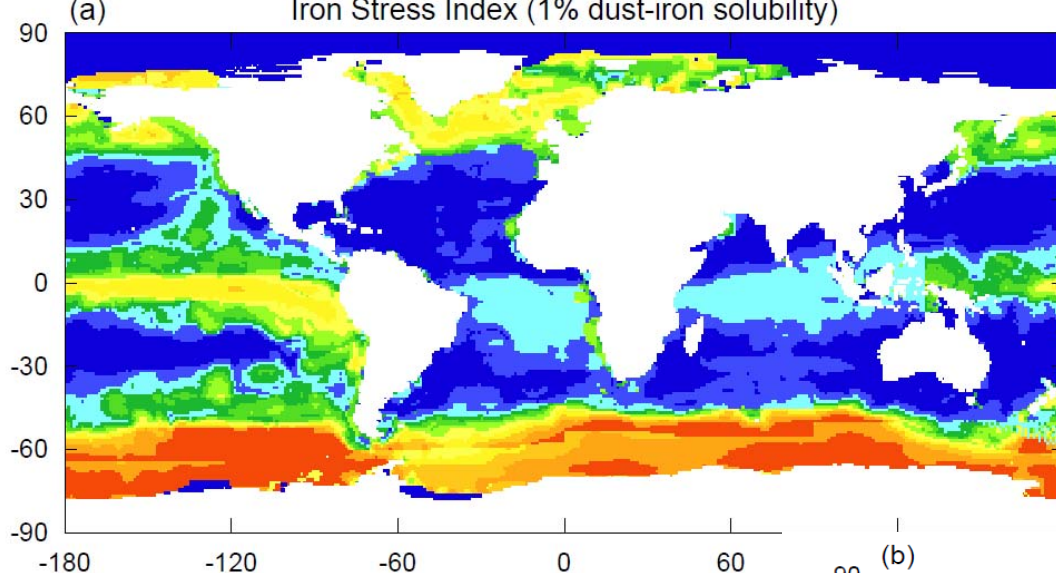


From Philip Boyd, New Zealand National Institute for Water and Atmospheric Research



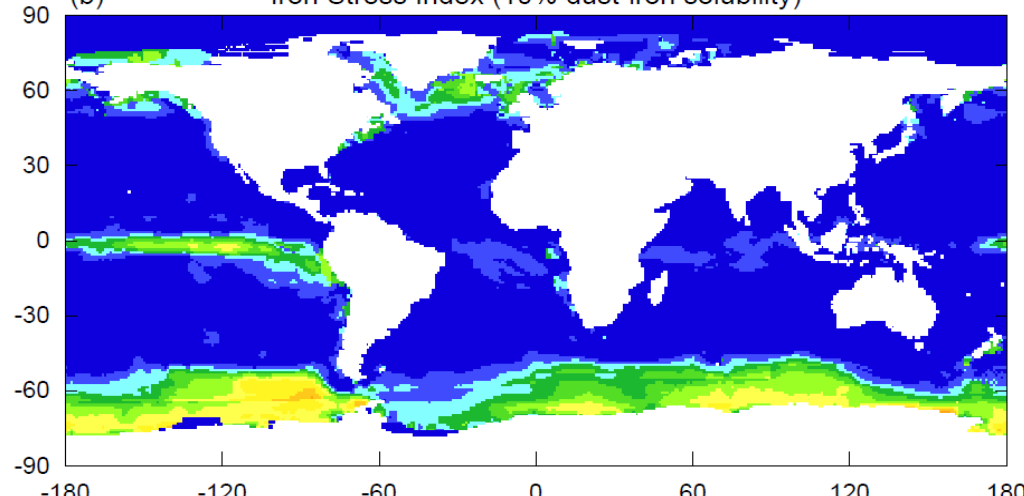
# What is a “Target” Dust Fe Solubility?

(a) Iron Stress Index (1% dust-iron solubility)



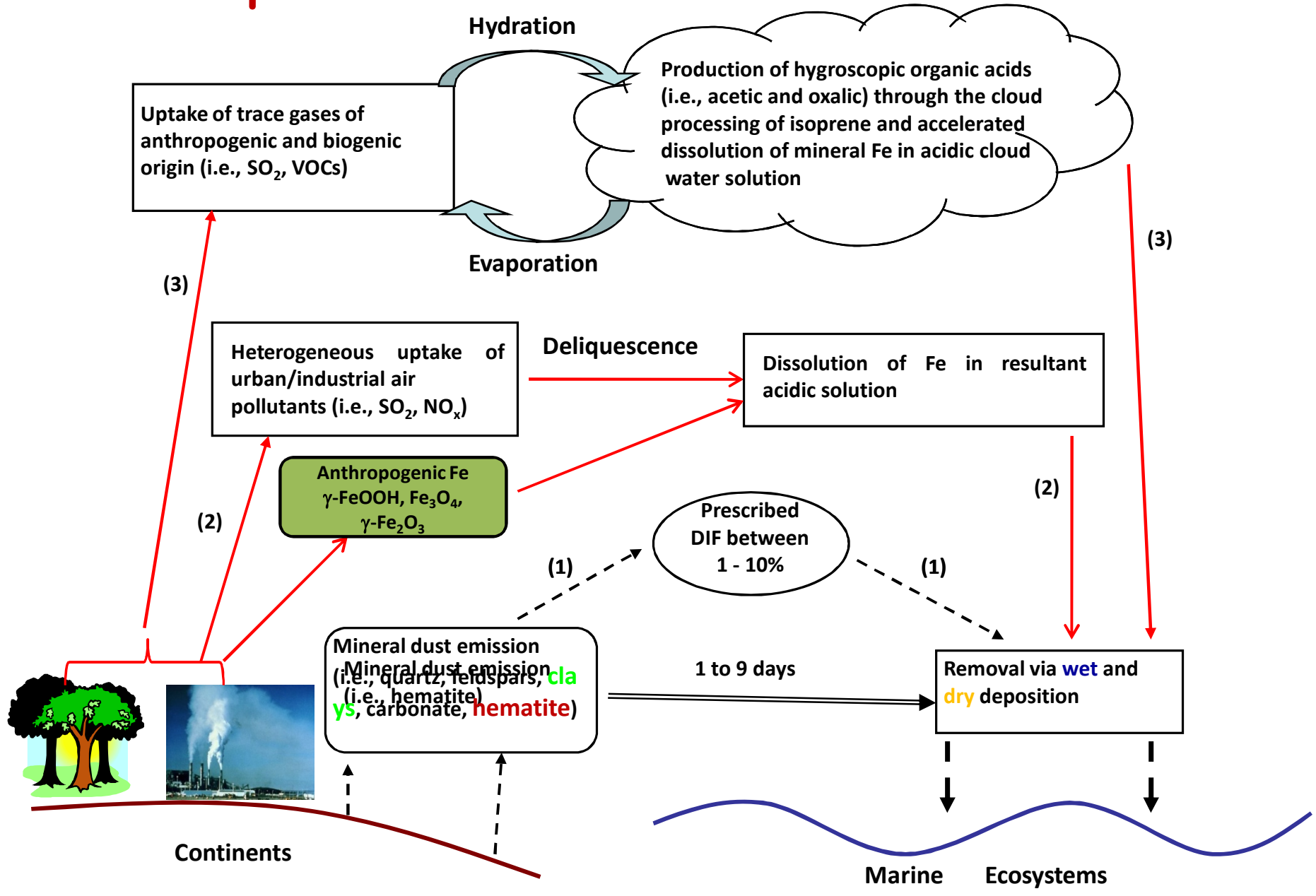
$$S = \frac{(\text{Fe:N})_{\text{cell}}}{(\text{Fe:N})_{\text{supplied}}}$$

(b) Iron Stress Index (10% dust-iron solubility)

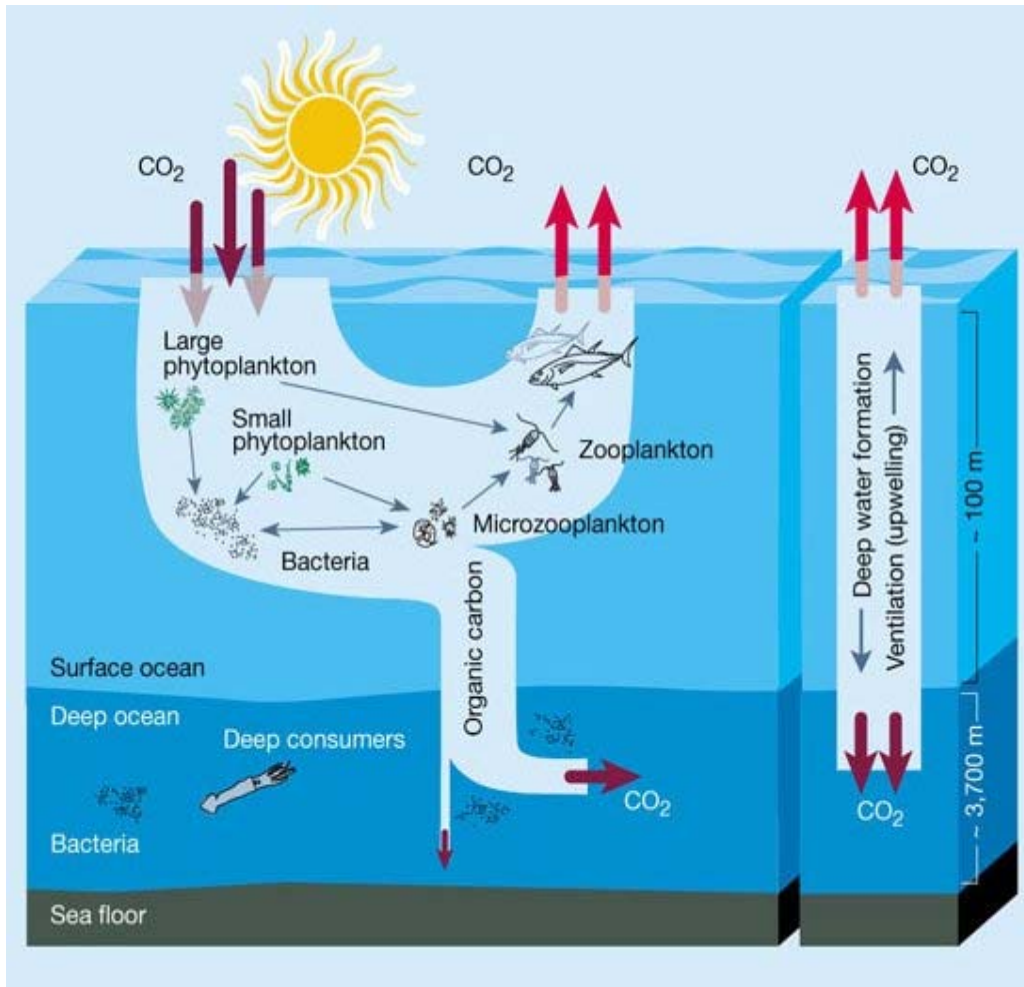


[Source: Fung, et al., 2000, GBC]

# The Main Pathways of Atmospheric Transport and Deposition of Soluble Fe to the Oceans



## Motivation #1 ( $CO_2$ -Climate Link)



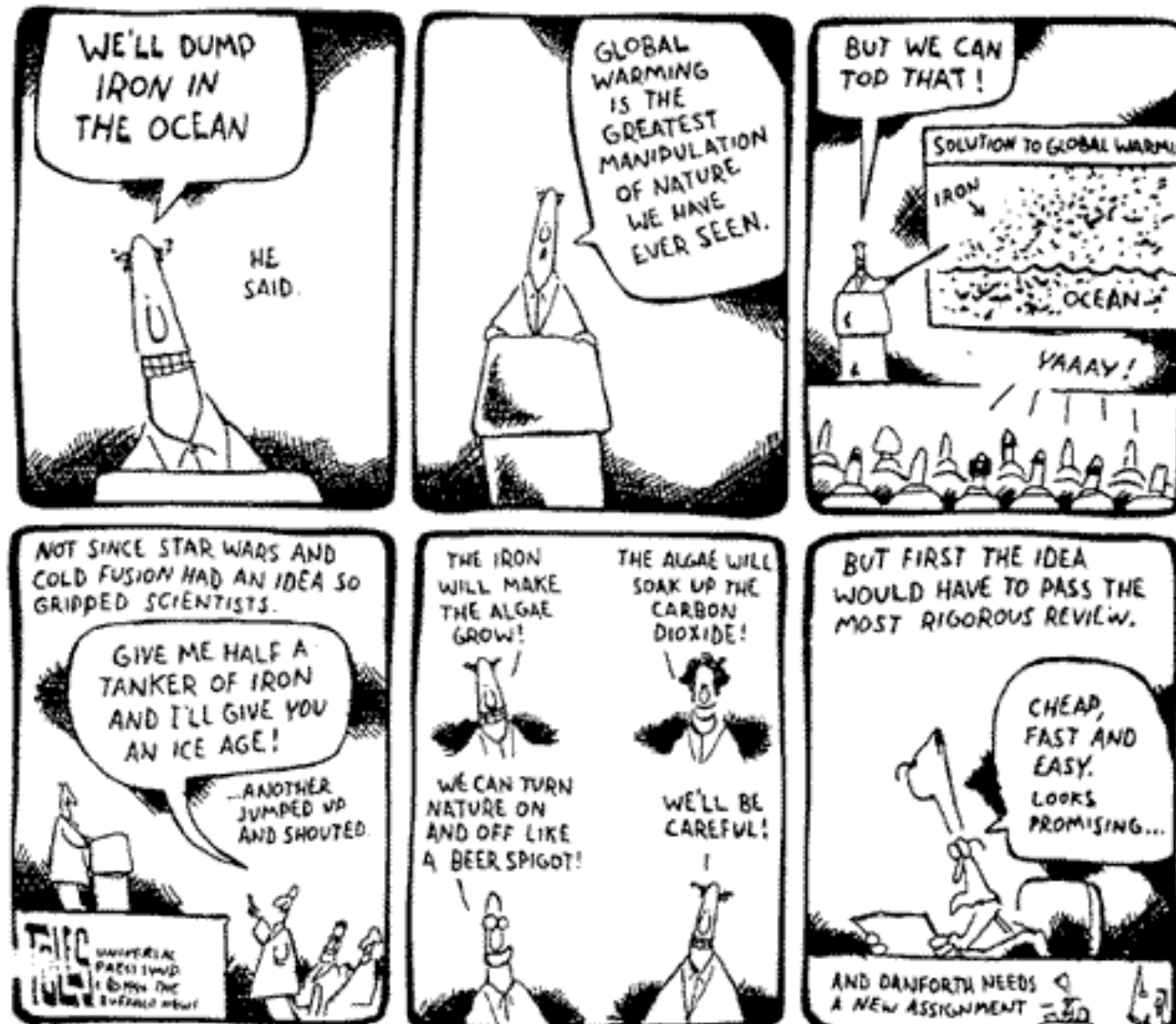
[Source: Chisholm, 2000, Nature.]

The “biological pump” is a collective property of a complex phytoplankton-based food web. Together with the “solubility pump”, it maintains a sharp gradient of CO<sub>2</sub> between the atmosphere and the deep oceans.

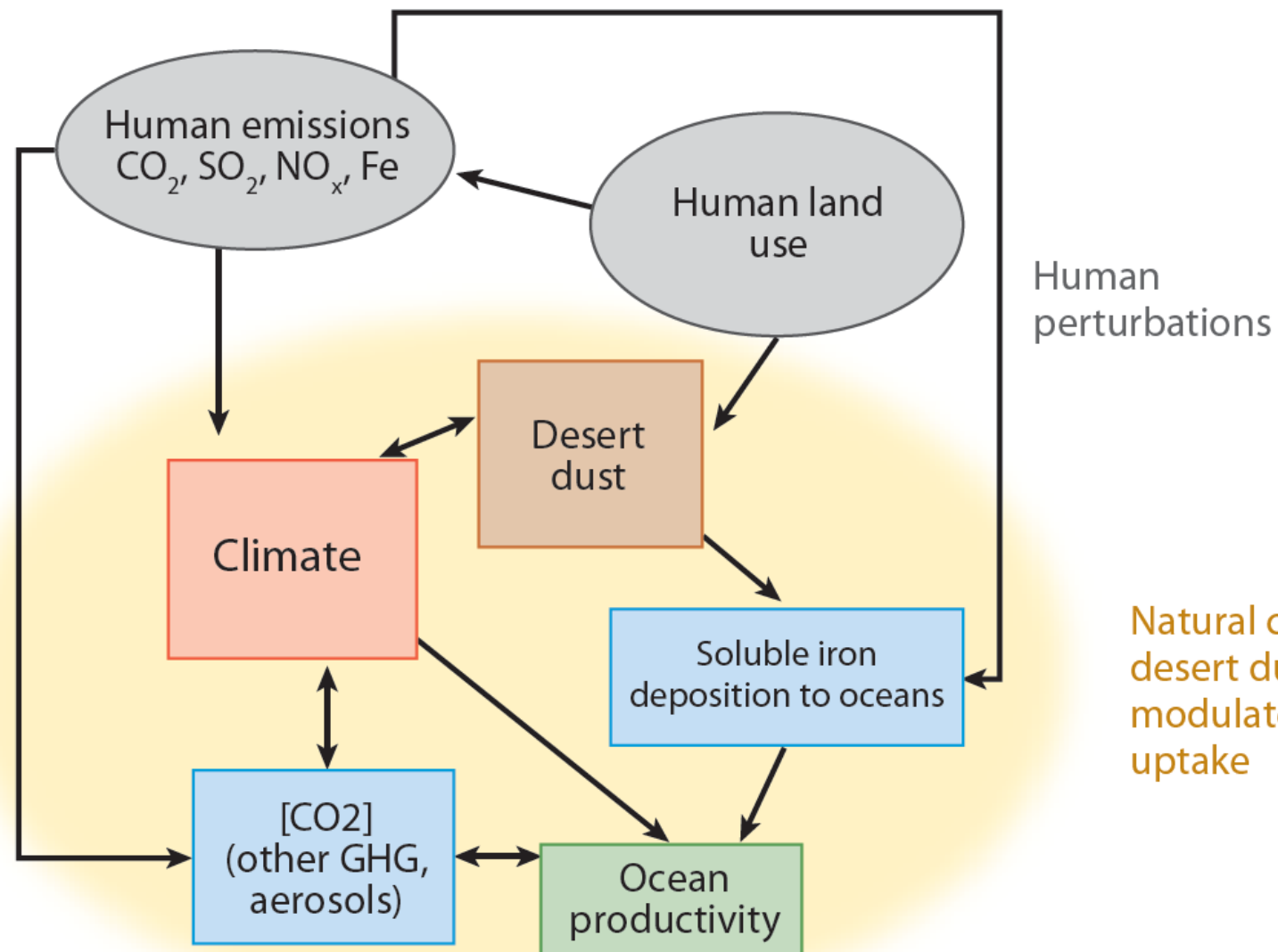


Plankton collage - Credit Collage by Mary Wilcox Silver, University of California, Santa Cruz

# The Iron Hypothesis



## Motivation #1 (continued)

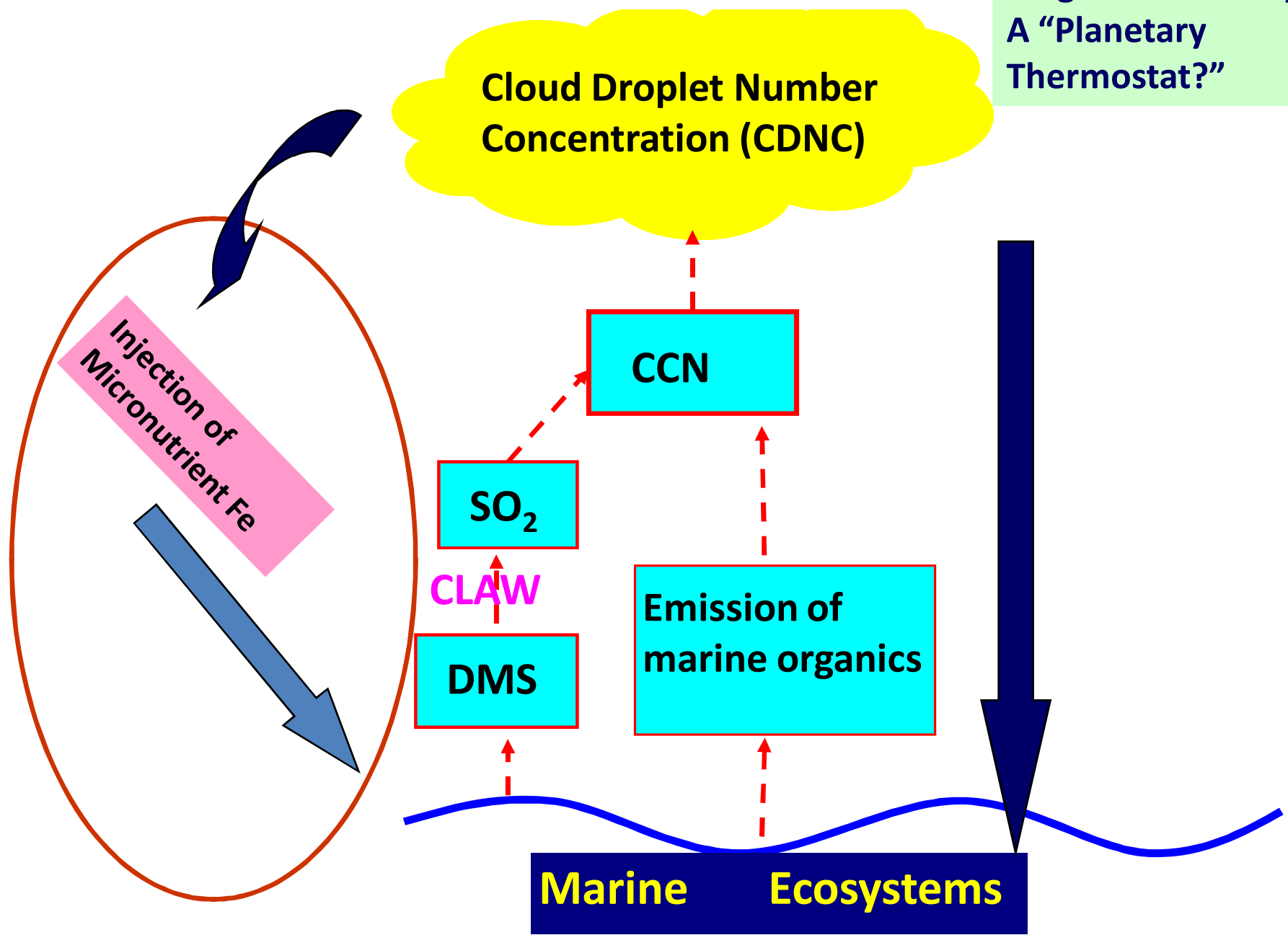


Natural cycle of how  
desert dust iron may  
modulate ocean  $\text{CO}_2$   
uptake

[Source: Mahowald, et  
al., 2009, Annu. Rev. Mar. Sci.]

## Motivation #2 (CCN-Climate Link)

Marine  
biogeochemical cycle:  
A “Planetary  
Thermostat?”



# Overview



- 1) Introduction & motivation
- 2) Acid dissolution of iron in mineral dust aerosols
- 3) Lagrangian equilibrium model
- 5) Other mechanisms for iron dissolution
- 4) Case studies using GEOS-Chem/DFeS

# Nomenclature

## Mineral Iron

Iron in dust – mainly in the form of Fe(III) oxides and clays

## Anthropogenic Iron

Iron from industrial emissions and biomass burning

## Dissolved Iron ( $\text{Fe}_{\text{dis}}$ ) Fe(II) and Fe(III)

Also Fe-sulfate and Fe-oxalate complexes

## Bioavailable iron

Dissolved-Fe + Leachable-Fe + some colloidal forms

## Thermodynamics vs. Kinetics

- ✓ Thermodynamics can tell you only that a reaction should go because the products are more stable (have a lower free energy) than the reactants.
- ✓ Says nothing about what rate (how fast) the reaction will be

In a spontaneous reaction,  $\Delta G$  (change in Gibbs free energy) is negative.

$\Delta G$  is largely dependent on two concepts:  $\Delta G = \Delta H - T\Delta S$ .

Enthalpy :  $\Delta H$ . Negative values of this (i.e. exothermic) decrease  $\Delta G$ , making the reaction more favorable.

Entropy :  $-T\Delta S$ . The  $T$  represents temperature. The  $S$  represents entropy, or a measurement of disorder. This term in the equation is negative and temperature is always positive. Therefore, increasing the change in entropy (positive  $\Delta S$ ) makes the reaction more favorable.



$$K = \frac{[C]^c [D]^d}{[A]^a [B]^b}$$

- ✓ The equilibrium constant, K, is a thermodynamic quantity. As such, it depends *only* on the overall reaction.

Notice, I have never mentioned time!!

- ✓ The rate of the reaction has no dependence on the overall reaction equation but instead depends on the reaction mechanism, the elementary steps.

Slow reaction



Fast reaction



# Mineral Dissolution Kinetics

$$R_i^{\text{net}} = K_r(T)a(H^+)^m f(\Delta G_r) A_i W_i$$

$R_i^{\text{net}}$  - The rate of dissolution of mineral  $i$  [mole dissolved/gram of dust/s]

$R_i^{\text{net}}$  >0 dissolution, <0 precipitation

$K_r$  - Dissolution constant [mole dissolved/m<sup>2</sup> of mineral/s]

$T$  - Temperature [K]

$a(H^+)$  - H<sup>+</sup> activity; pH=-log{H<sup>+</sup>}

$m$  - An empirical parameter

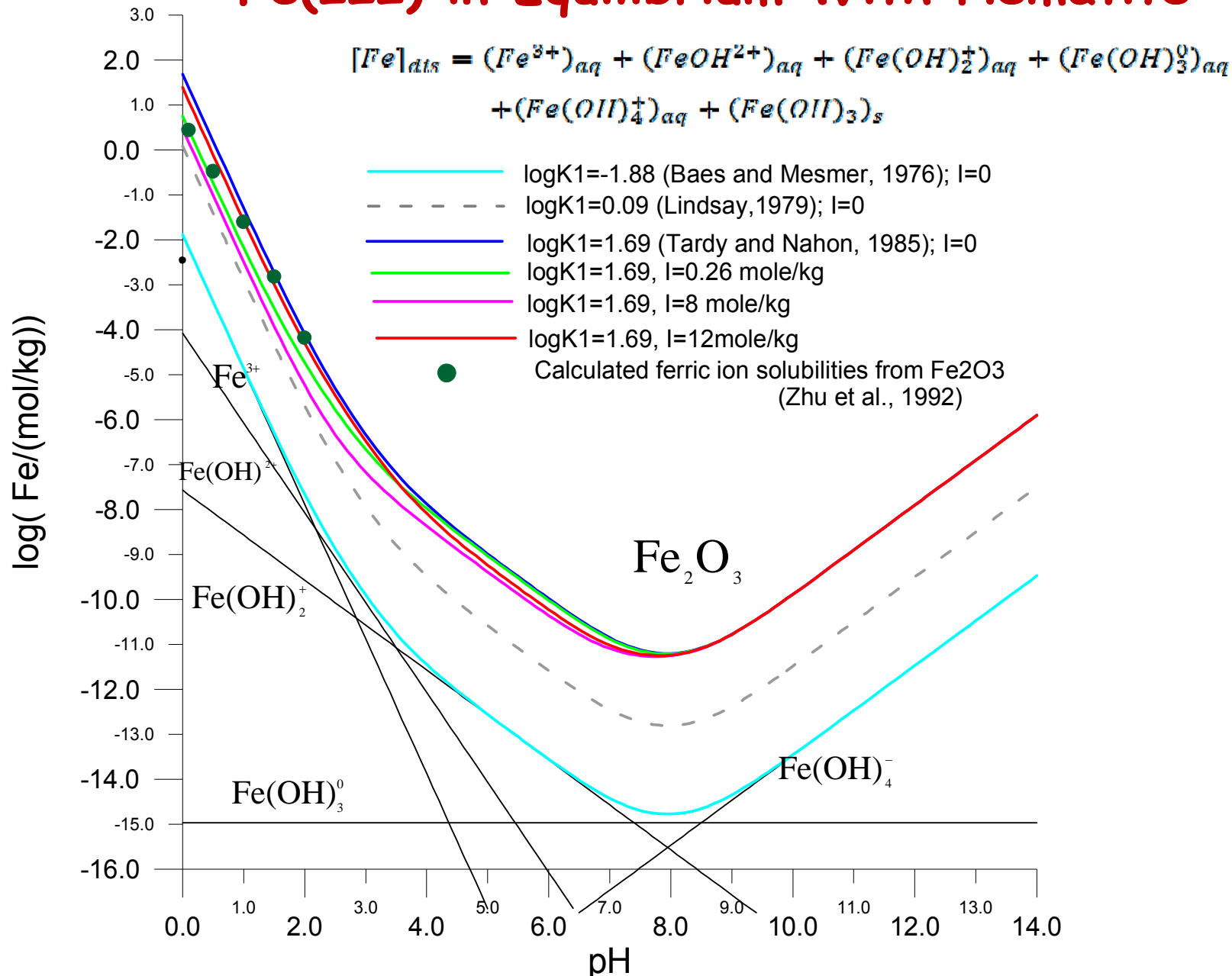
$f$  - A function of Gibbs Free energy,  $\Delta G_r$

$$f(\Delta G_r) = [1 - \exp(n\Delta G_r/RT)] \quad \Delta G_r = RT \ln(Q/K_{\text{eq}})$$

$A_i$  - Specific surface area of mineral [m<sup>2</sup>/g of mineral]

$W_i$  - Weight fraction of the mineral in dust [g of mineral/g of dust]

# Concentrations of Different Hydrolysis Species of Fe(III) in Equilibrium With Hematite



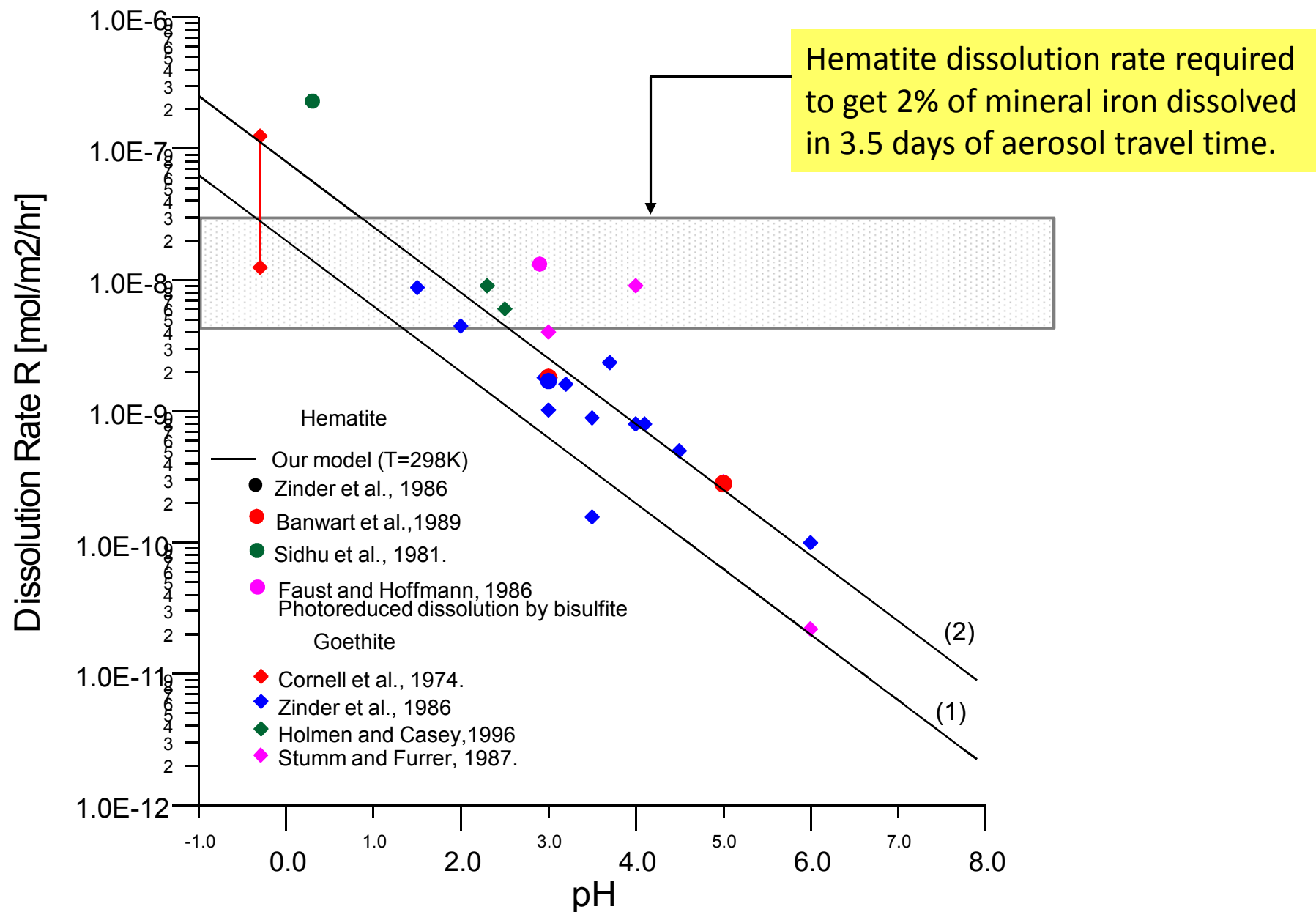
# Mineral Dissolution Kinetics

**Table 8.** Constants Used to Calculate Mineral Dissolution/Precipitation Rates Using Equation (22)

No.	Mineral	Rate Constant $K_r$ (mol <sub>mineral dissolved</sub> /m <sup>2</sup> /s)	m	A <sub>i</sub> , m <sup>2</sup> g <sup>-1</sup>	W <sub>i</sub> g(Mineral)/ g(Dust) x 100%	Source
RS1	calcite	$7.0 \times 10^{-2} \exp[1200(1/298-1/T)]$	1	0.1	11	<i>Morse and Arvidson [2002]; Alkattan et al. [1998]; Chou et al. [1988]; Sjöberg [1976]</i>
RS2	albite	$2.4 \times 10^{-10} \exp[7200(1/298-1/T)]$	0.5	1.0	17	<i>Blum and Stilling [1995]; Hodson [1999]</i>
RS3	microcline	$2.0 \times 10^{-10} \exp[6600(1/298-1/T)]$ <sup>(1)</sup>	0.5	1.0	8	<i>Blum and Stilling [1995]; Hodson [1999]</i>
RS4	illite	$1.3 \times 10^{-11} \exp[6700(1/298-1/T)]$ <sup>(1)</sup>	0.39	90	20	<i>Nagy [1995]; Tessier [1990]; Skopp [2000]</i>
RS5	smectite	$8.1 \times 10^{-12} \exp[6700(1/298-1/T)]$ <sup>a</sup>	0.3	300	8	<i>Nagy [1995]; Tessier [1990]; Skopp [2000]</i>
RS6	kaolinite	$4 \times 10^{-11} \exp[6700(1/298-1/T)]$	0.1	20	5	<i>Carroll and Walter [1990]; Nagy [1995]; Skopp [2000]</i>
RS7	hematite	stage I (0 to 0.8% of total oxide dissolved) $4.4 \times 10^{-12} \exp[9.2 \times 10^3(1/298-1/T)]$ stage II (0.8 to 40% of total oxide dissolved) $1.8 \times 10^{-11} \exp[9.2 \times 10^3(1/298-1/T)]$ stage III (40 to 100% of total oxide dissolved) $3.5 \times 10^{-12} \exp[9.2 \times 10^3(1/298-1/T)]$	0.5	100	5	<i>Azuma and Kametani [1964]; Blesa et al. [1994]; Cornell and Schwertmann [1996]; Zinder et al. [1986]; Skopp [2000]</i>

<sup>a</sup>Average activation energy for kaolinite [Carroll and Walter, 1990] is used.

# Summary of Several Experimental Results for the Rates of Hematite and Goethite Dissolution



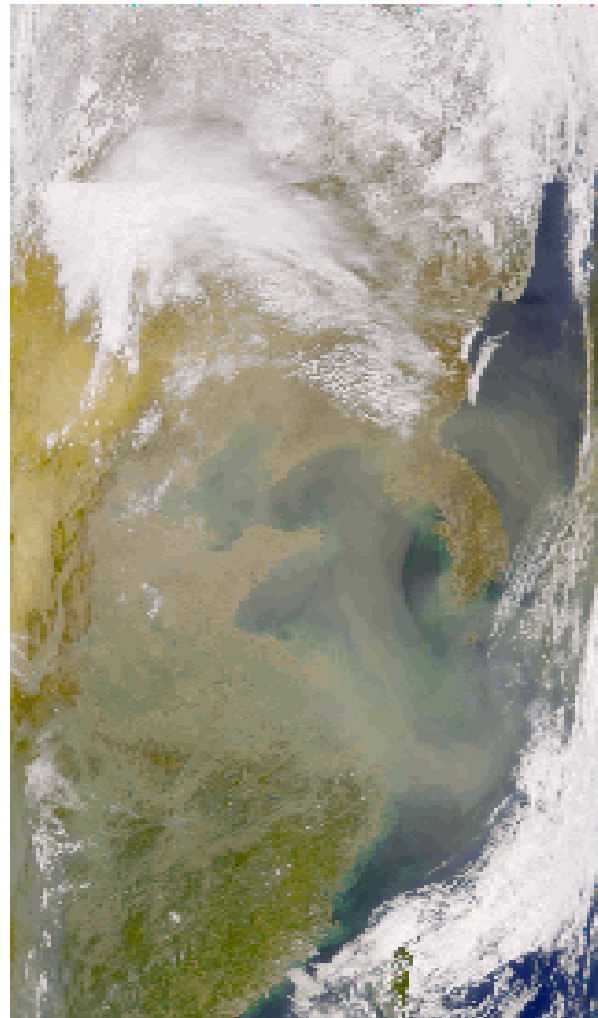
# The “Acid-mobilization” Hypothesis



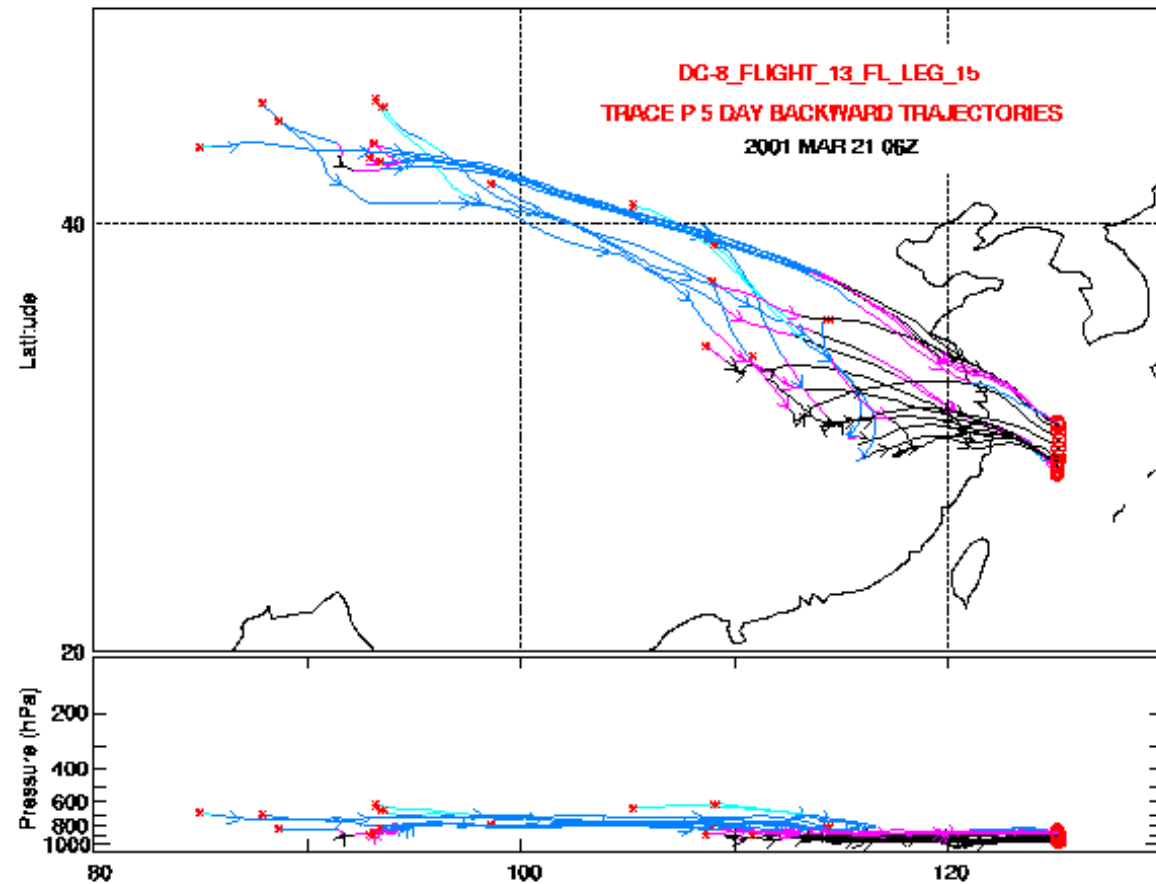
Fe in mineral dust is mobilized during transport in the atmosphere in a two-step process consisting of:

- (1) *acidification of the mineral dust by the incorporation of acids arising from air pollutants (and in particular SO<sub>2</sub>) that are mixed into the plumes containing dust as these plumes advect over the urban and industrial centers;*
- (2) *dissolution of the Fe in the resultant acidic solutions.*

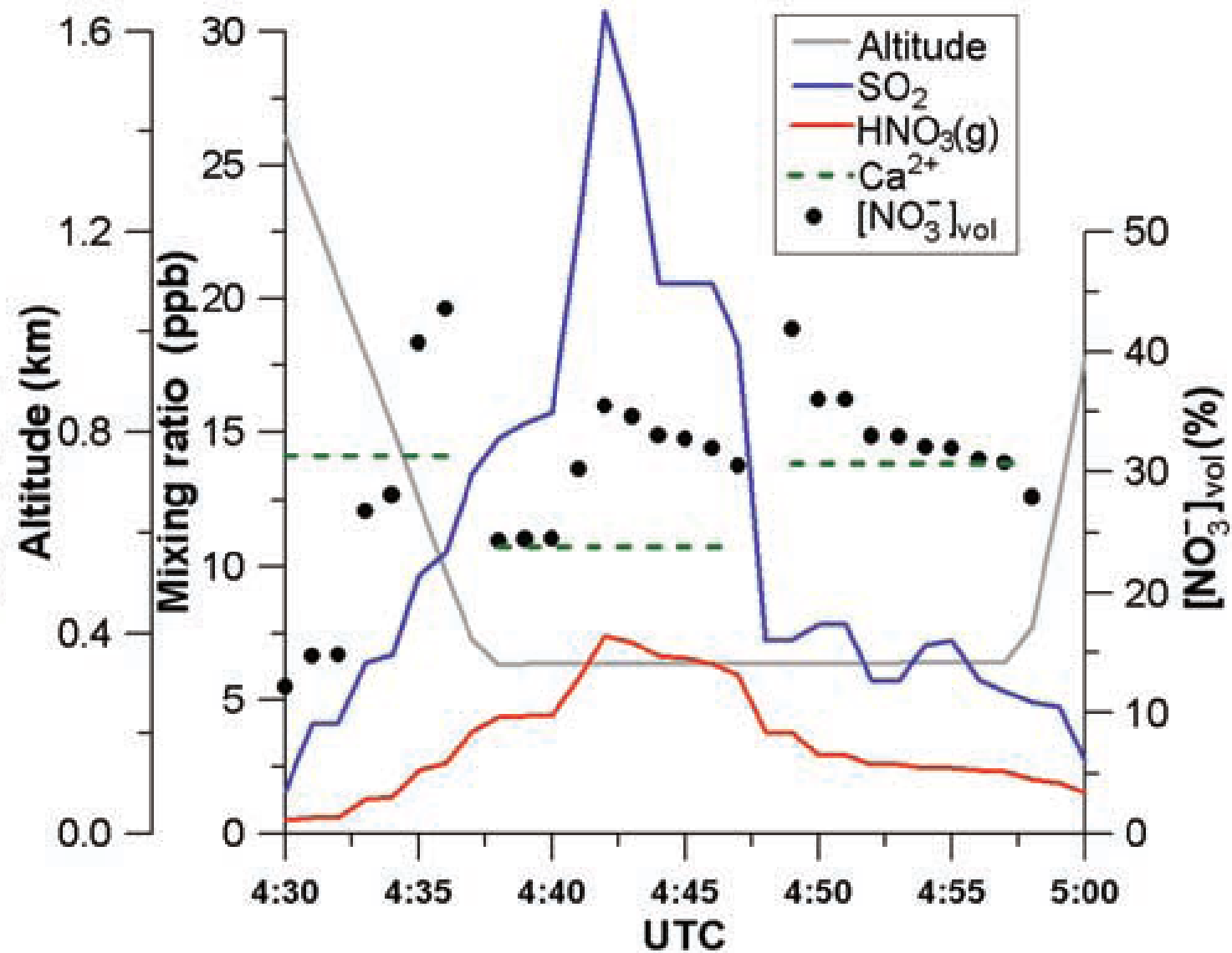
# Evidence for the “Acidic Dust?”



Orbview-2 SeaWiFS TrueColor  
UCAR/JOSS 2001/03/21 04:14 UTC

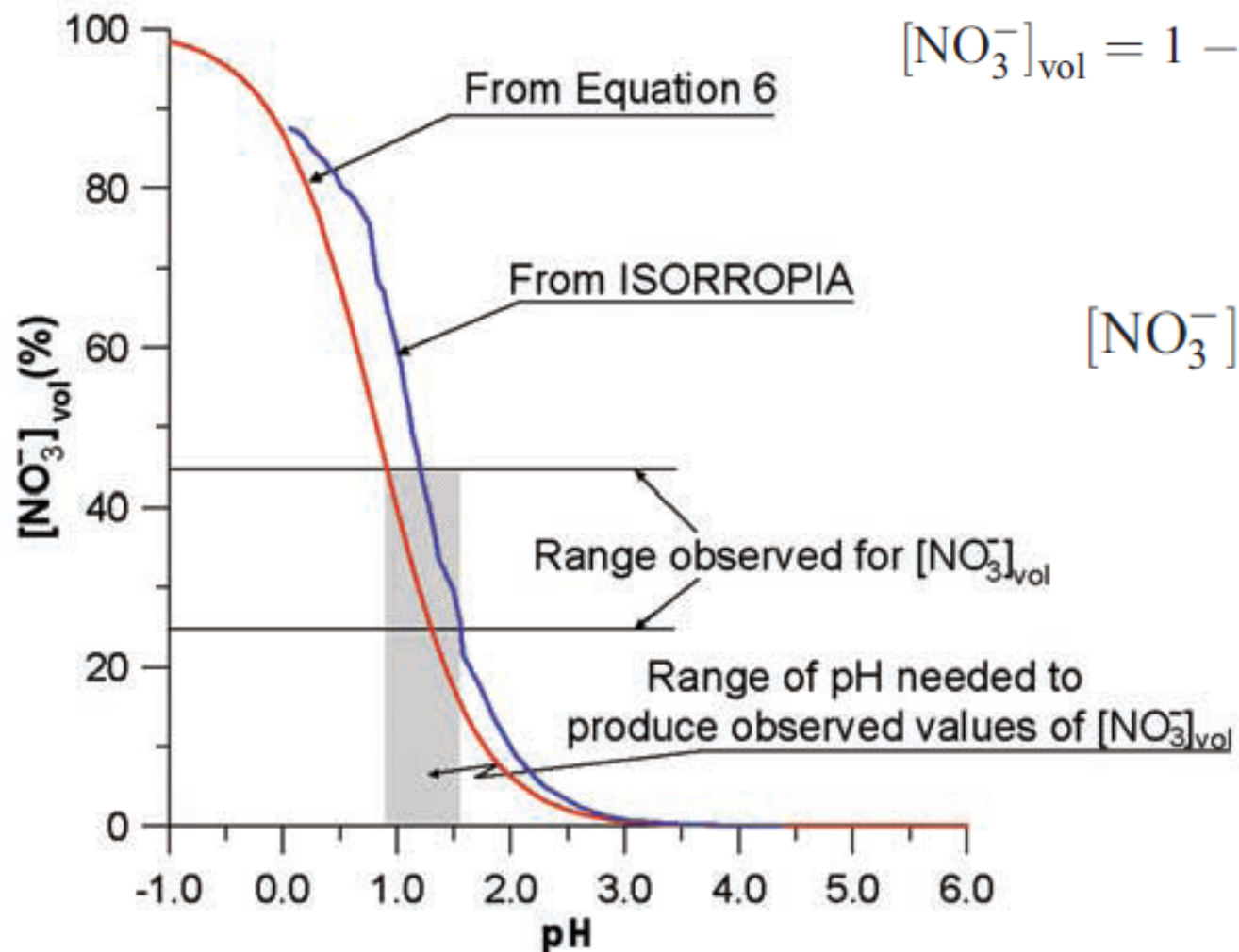


## Evidence for the “Acidic Dust?” (continued)



[Source: Meskhidze et al., GRL, 2003]

# Nitrate Volatilization

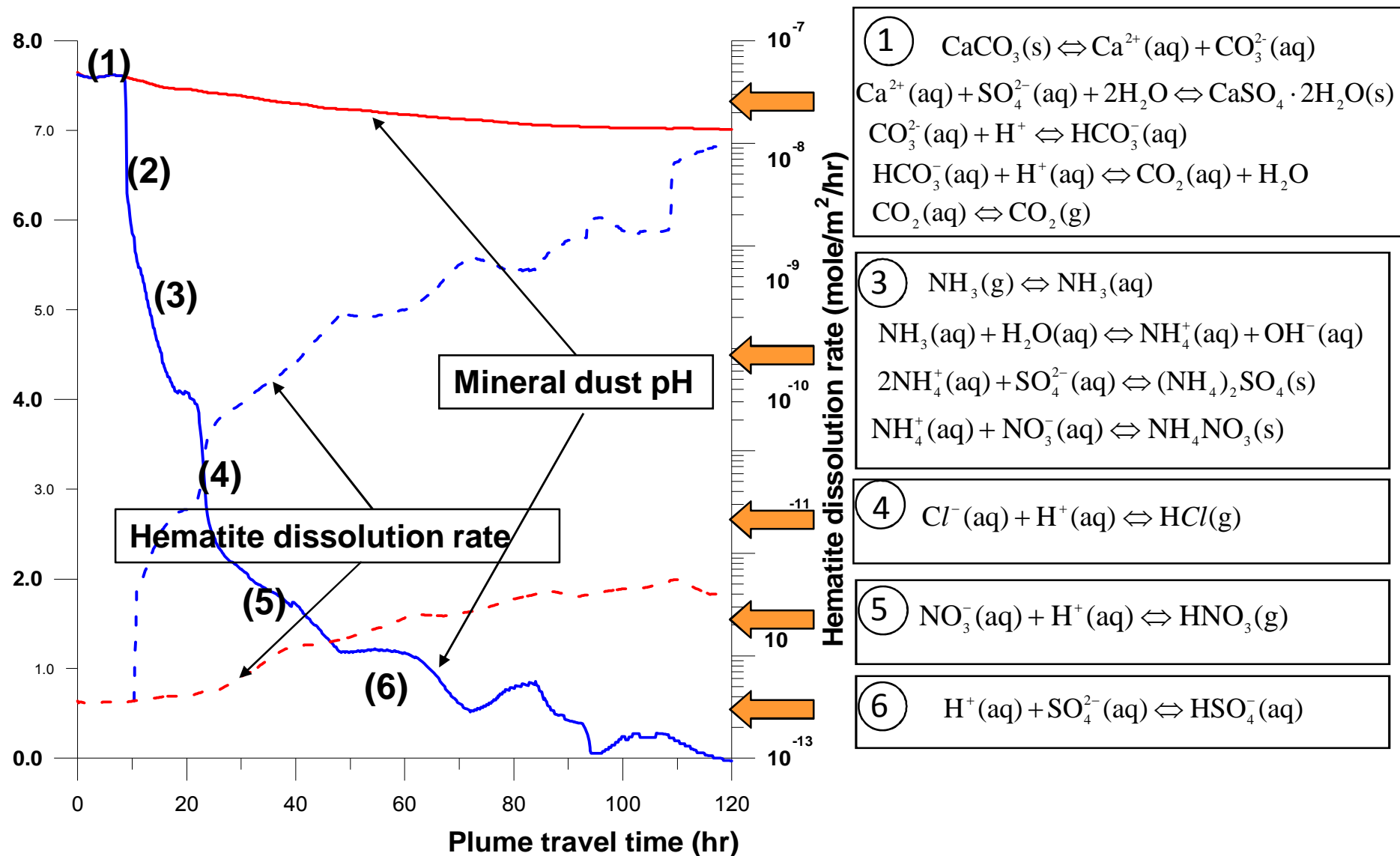


$$[NO_3^-]_{vol} = 1 - \frac{[NO_3^-]}{[NO_3^-] + [HNO_3(g)]}$$

$$[NO_3^-]_{vol} = \frac{[H^+]}{[H^+] + K}$$

[Source: Meskhidze et al., GRL, 2003]

# Mineral Aerosol and Acidic Trace Gases



# Overview



- 1) Introduction & motivation
- 2) Acid dissolution of iron in mineral dust aerosols
- 3) Lagrangian equilibrium model
- 4) Other mechanisms for iron dissolution
- 5) Case studies using GEOS-Chem/DFeS

# Lagrangian Equilibrium Model

## Anthropogenic Mode

### Liquid phase

$\text{H}^+$ ,  $\text{NH}_4^+$ ,  $\text{SO}_4^{2-}$ ,  $\text{HSO}_4^-$ ,  $\text{NO}_3^-$ ,  $\text{Cl}^-$ ,  $\text{K}^+$ ,  $\text{Na}^+$

### Solid phase

$\text{NaCl}$ ,  $\text{NaNO}_3$ ,  $\text{Na}_2\text{SO}_4$ ,  $\text{NaHSO}_4$ ,  $\text{NH}_4\text{Cl}$ ,  $\text{NH}_4\text{NO}_3$ ,  $(\text{NH}_4)_2\text{SO}_4$ ,  $\text{NH}_4\text{HSO}_4$ ,  $(\text{NH}_4)_3\text{H}(\text{SO}_4)_2$

## Gas phase

NH<sub>3</sub>  
HCl  
HNO<sub>3</sub>  
SO<sub>2</sub>  
NO  
O<sub>3</sub>  
NO<sub>2</sub>

## Dust Mode

### Liquid phase

$\text{H}^+$ ,  $\text{NH}_4^+$ ,  $\text{SO}_4^{2-}$ ,  $\text{HSO}_4^-$ ,  $\text{NO}_3^-$ ,  $\text{Cl}^-$ ,  $\text{K}^+$ ,  $\text{Na}^+$ ,  $\text{Ca}^{2+}$ ,  $\text{Mg}^{2+}$ ,  $\text{Fe}^{3+}$ ,  $\text{Fe(OH)}^{2+}$ ,  $\text{Fe(OH)}_2^+$ ,  $\text{Fe(OH)}_3^0$ ,  $\text{Fe(OH)}_4^-$ ,  $\text{FeSO}_4^+$

### Solid phase

$\text{NaCl}$ ,  $\text{NaNO}_3$ ,  $\text{Na}_2\text{SO}_4$ ,  $\text{CaCO}_3$ ,  $\text{CaSO}_4$ ,  $\text{NaHSO}_4$ ,  $\text{NH}_4\text{Cl}$ ,  $\text{NH}_4\text{NO}_3$ ,  $(\text{NH}_4)_2\text{SO}_4$ ,  $\text{NH}_4\text{HSO}_4$ ,  $\text{Fe}_2\text{O}_3$ ,  $(\text{NH}_4)_3\text{H}(\text{SO}_4)_2$ ,  $\text{NaAlSi}_3\text{O}_8$ ,  $\text{KAlSi}_3\text{O}_8$ ,  $\text{Fe(OH)}_3(s)$ , illite, smectite

$$R_{\text{net}} = k_0 \exp\left(\frac{-E_{\text{app}}}{RT}\right) a_{\text{H}^+}^{m_{\text{H}^+}} \prod_i a_i^{m_i} g_i(l) f(\Delta G_r)$$

Consider **pH**, **temperature**, **ionic strength** of the solution and **specific surface area** of minerals

# Iron Dissolution Modeling



1: Initial mineral composition for the dust



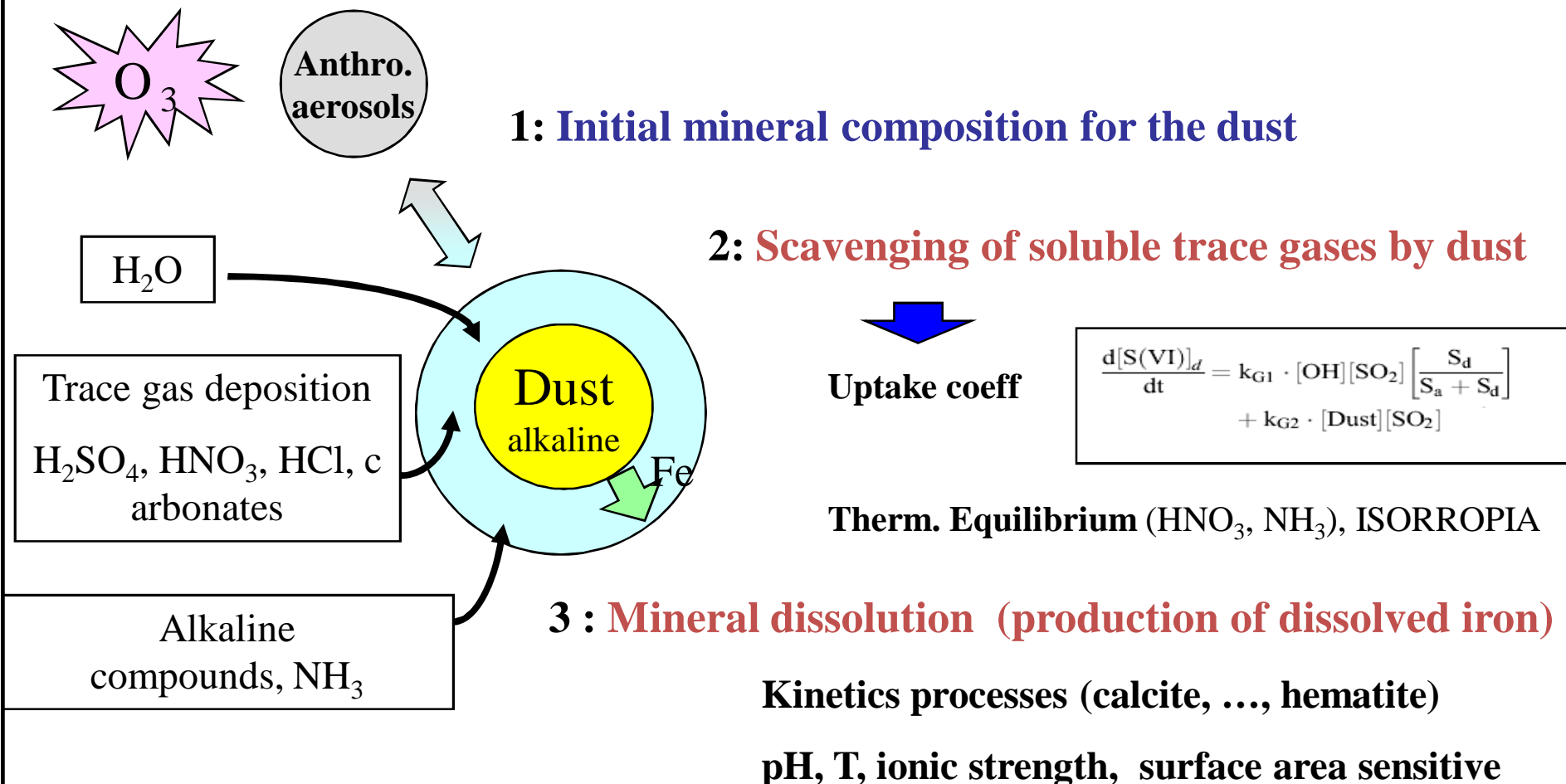
# Iron Dissolution Modeling

Minerals	<u>In Soil, % wt<sup>a</sup></u>	
	In Silt	In Clay
Anhydrite $\text{CaSO}_4$	6 <sup>+</sup>	0
Calcite $\text{CaCO}_3$	4	0 <sup>+</sup>
Plagioclase Albite – $\text{NaAlSi}_3\text{O}_8$ Microcline – $\text{KAlSi}_3\text{O}_8$	28	8
Illite $\text{K}_{0.6}\text{Mg}_{0.25}\text{Al}_{2.3}\text{Si}_{3.5}\text{O}_{10}(\text{OH})_2$	18 <sup>+</sup>	13
Smeectite/Montmorillonite $\text{Na}_{0.6}\text{Al}_{1.4}\text{Mg}_{0.6}\text{Si}_4\text{O}_{10}(\text{OH})_2 \cdot 4\text{H}_2\text{O}$	7 <sup>+</sup>	62
Hematite $\text{Fe}_2\text{O}_3$	5	3
Quartz $\text{SiO}_2$	27	7
Kaolinite $\text{Al}_2\text{Si}_2\text{O}_5(\text{OH})_4$	5 <sup>+</sup>	7
<b>Total</b>	<b>100</b>	<b>100</b>

<sup>a</sup> Mineralogical composition were largely based on Gaiero et al. (2003), Smith et al. (2003), and Ramsperger et al. (1998).

<sup>+</sup> Assumed generic dust composition due to insufficient data.

# Iron Dissolution Modeling



# Iron Dissolution Modeling

**Table 7.** Equilibria Describing the Dissolution/Precipitation of Minerals Contained in Dust

No.	Equilibrium Reaction	Equilibrium Constants <sup>a</sup>		Source
		$K_{eq}$ , mol <sup>2</sup> /kg <sup>2</sup>		
REQ1	calcite $\rightleftharpoons$ Ca <sup>2+</sup> + CO <sub>3</sub> <sup>2-</sup>	4.959 × 10 <sup>-9</sup>		Meng et al. [1995]
REQ2	albite + 4H <sup>+</sup> + 4H <sub>2</sub> O $\rightleftharpoons$ Na <sup>+</sup> + Al <sup>3+</sup> + 3H <sub>4</sub> SiO <sub>4</sub> <sup>0</sup>	1.6 × 10 <sup>3</sup>		Lindsay [1979]
REQ3	microcline + 4H <sup>+</sup> + 4H <sub>2</sub> O $\rightleftharpoons$ K <sup>+</sup> + Al <sup>3+</sup> + 3H <sub>4</sub> SiO <sub>4</sub> <sup>0</sup>	1 × 10 <sup>1</sup>		Lindsay [1979]
REQ4	illite + 6H <sup>+</sup> + 4H <sub>2</sub> O $\rightleftharpoons$ 0.4K <sup>+</sup> + 0.25Mg <sup>2+</sup> + 1.7Al <sup>3+</sup> + 4H <sub>4</sub> SiO <sub>4</sub> <sup>0</sup>	2.24 × 10 <sup>10</sup>		Lindsay [1979]
REQ5	smectite + 4H <sup>+</sup> $\rightleftharpoons$ 0.8Na <sup>+</sup> + 0.4Mg <sup>2+</sup> + 0.8Al <sup>3+</sup> + 4H <sub>4</sub> SiO <sub>4</sub> <sup>0</sup>	4.79 × 10 <sup>2</sup>		Lindsay [1979]
REQ6	kaolinite + 6H <sup>+</sup> $\rightleftharpoons$ 2Al <sup>3+</sup> + 2H <sub>4</sub> SiO <sub>4</sub> <sup>0</sup> + H <sub>2</sub> O	2.8 × 10 <sup>5</sup>		Lindsay [1979]
REQ7	hematite + 6H <sup>+</sup> $\rightleftharpoons$ 2Fe <sup>3+</sup> + 3H <sub>2</sub> O	4.4 × 10 <sup>-1</sup>		Blesa et al. [1994]

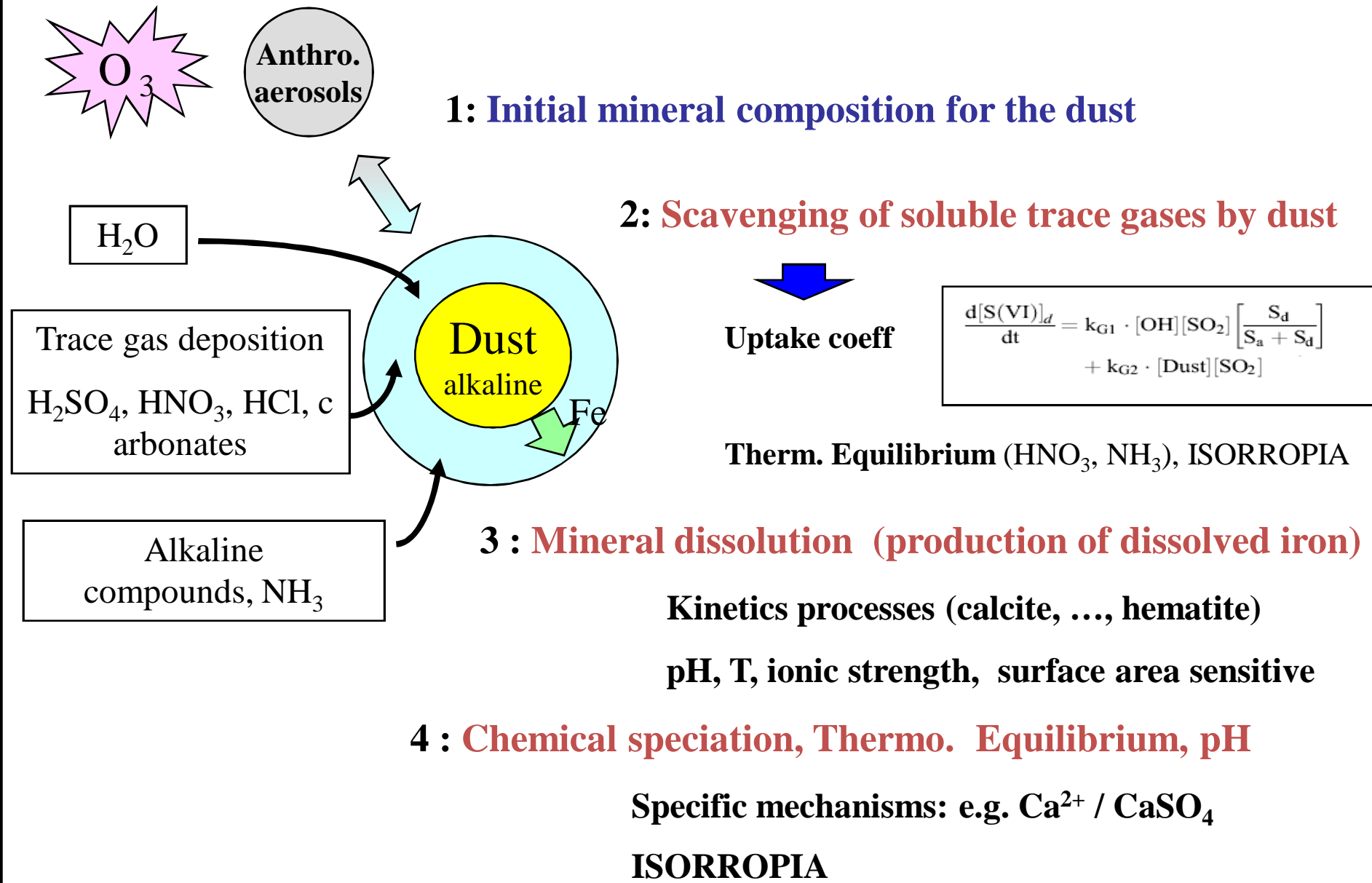
<sup>a</sup>All  $K_{eq}$  values are for 298 K.

**Table 8.** Constants Used to Calculate Mineral Dissolution/Precipitation Rates Using Equation (22)

No.	Mineral	Rate Constant $K_r$ (mol <sub>mineral dissolved</sub> /m <sup>2</sup> /s)	m	A <sub>i</sub> , m <sup>2</sup> g <sup>-1</sup>	W <sub>i</sub> g(Mineral)/ g(Dust)	Source
RS1	calcite	$7.0 \times 10^{-2} \exp[1200(1/298-1/T)]$	1	0.1	11	Morse and Arvidson [2002]; Alkattan et al. [1998]; Chou et al. [1988]; Sjöberg [1976]
RS2	albite	$2.4 \times 10^{-10} \exp[7200(1/298-1/T)]$	0.5	1.0	17	Blum and Stilling [1995]; Hodson [1999]
RS3	microcline	$2.0 \times 10^{-10} \exp[6600(1/298-1/T)]$ <sup>(1)</sup>	0.5	1.0	8	Blum and Stilling [1995]; Hodson [1999]
RS4	illite	$1.3 \times 10^{-11} \exp[6700(1/298-1/T)]$ <sup>(1)</sup>	0.39	90	20	Nagy [1995]; Tessier [1990]; Skopp [2000]
RS5	smectite	$8.1 \times 10^{-12} \exp[6700(1/298-1/T)]$ <sup>a</sup>	0.3	300	8	Nagy [1995]; Tessier [1990]; Skopp [2000]
RS6	kaolinite	$4 \times 10^{-11} \exp[6700(1/298-1/T)]$	0.1	20	5	Carroll and Walter [1990]; Nagy [1995]; Skopp [2000]
RS7	hematite	stage I (0 to 0.8% of total oxide dissolved) $4.4 \times 10^{-12} \exp[9.2 \times 10^3(1/298-1/T)]$ stage II (0.8 to 40% of total oxide dissolved) $1.8 \times 10^{-11} \exp[9.2 \times 10^3(1/298-1/T)]$ stage III (40 to 100% of total oxide dissolved) $3.5 \times 10^{-12} \exp[9.2 \times 10^3(1/298-1/T)]$	0.5	100	5	Azuma and Kametani [1964]; Blesa et al. [1994]; Cornell and Schwertmann [1996]; Zinder et al. [1986]; Skopp [2000]

[Source: Meskhidze et al., JGR, 2005]

# Iron Dissolution Modeling



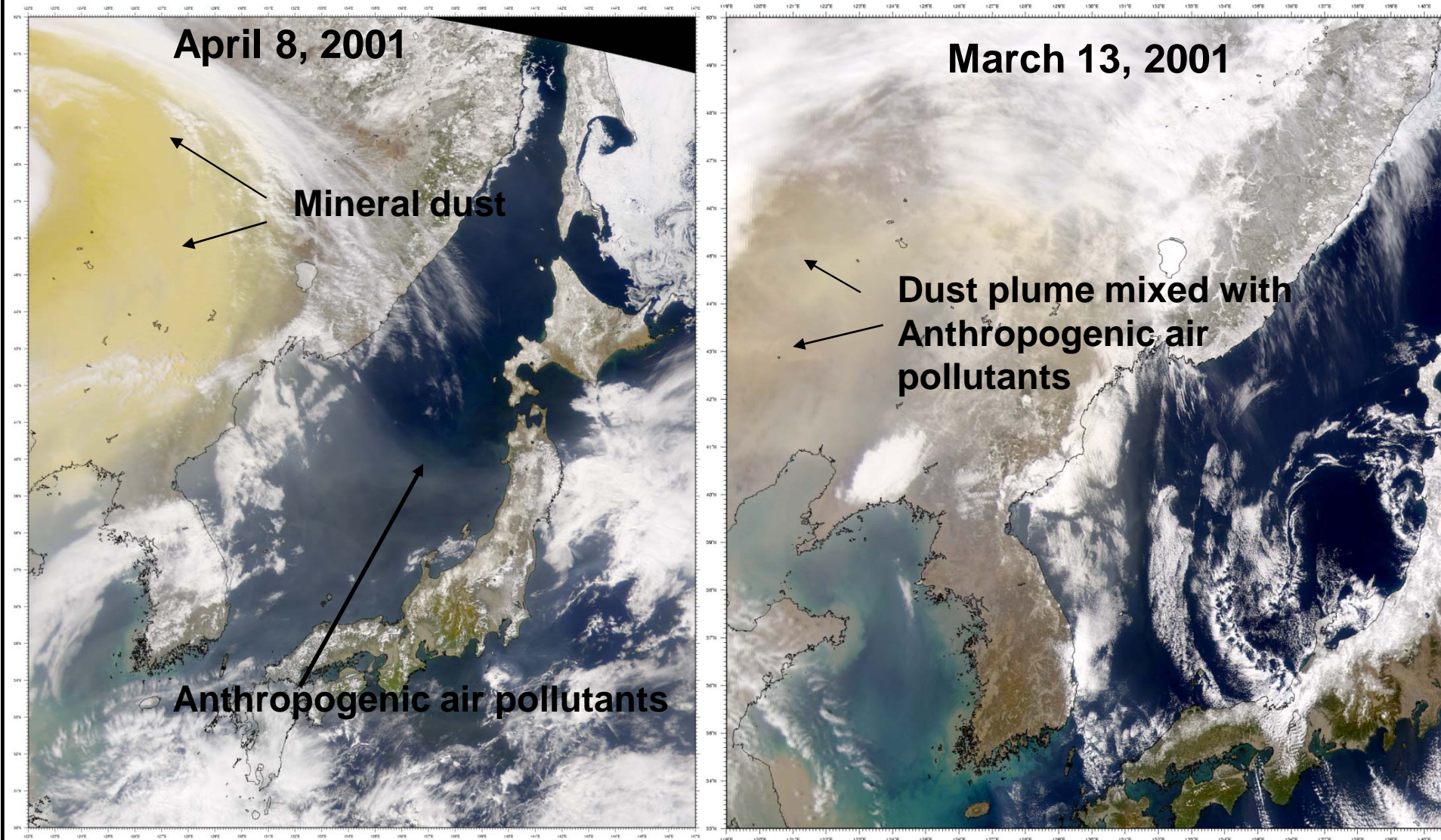
# Iron Dissolution Modeling

**Table 6.** Additional Aqueous-Phase Reactions Added to Modified Version of ISORROPIA and Their Equilibrium Constants

No.	Equilibrium Reaction	Equilibrium Constants <sup>a</sup>				Source
		K° (298.15 K)	a	b	Units	
RAQ1	$\text{CO}_2(\text{aq}) \rightleftharpoons \text{CO}_2(\text{g})$	$3.404 \times 10^{-2}$	8.1858	-28.9307	mol/kg/atm	Meng et al. [1995]
RAQ2	$\text{HCO}_3^- + \text{H}^+ \rightleftharpoons \text{CO}_2(\text{aq})$	$4.299 \times 10^{-7}$	3.0821	31.8139	mol/kg	Meng et al. [1995]
RAQ3	$\text{CO}_3^{2-} + \text{H}^+ \rightleftharpoons \text{HCO}_3^-$	$4.678 \times 10^{-11}$	5.9908	38.8440	mol/kg	Meng et al. [1995]
RAQ4	$\text{CaSO}_4 \cdot 2\text{H}_2\text{O}(\text{s}) \rightleftharpoons \text{Ca}^{2+}(\text{aq}) + \text{SO}_4^{2-}(\text{aq}) + 2\text{H}_2\text{O}$	$K_{\text{eq}}$ $4.319 \times 10^{-5}$			$\text{mol}^2/\text{kg}^2$	Meng et al. [1995]
RAQ5	$\text{Fe(OH)}_3(\text{s}) + 3\text{H}^+ \rightleftharpoons \text{Fe}^{3+} + 3\text{H}_2\text{O}$	$9.1 \times 10^3$			mol/kg	Stumm and Morgan [1981]
RAQ6	$\text{Fe}^{3+} + \text{SO}_4^{2-} \rightleftharpoons \text{FeSO}_4^+$	$1.9 \times 10^4$			mol/kg	Millero et al. [1995]
RAQ7	$\text{FeCl}^{2+} \rightleftharpoons \text{Fe}^{3+} + \text{Cl}^-$	$1.9 \times 10^1$			mol/kg	Millero et al. [1995]
RAQ8	$\text{Fe}^{3+} + \text{H}_2\text{O} \rightleftharpoons \text{FeOH}^{2+} + \text{H}^+$	$6.46 \times 10^{-3}$			mol/kg	Stumm and Morgan [1981]
RAQ9	$\text{Fe}^{3+} + 2\text{H}_2\text{O} \rightleftharpoons \text{Fe(OH)}_2^+ + 2\text{H}^+$	$2.14 \times 10^{-6}$			mol/kg	Stumm and Morgan [1981]
RAQ10	$\text{Fe}^{3+} + 3\text{H}_2\text{O} \rightleftharpoons \text{Fe(OH)}_3^0 + 3\text{H}^+$	$1.59 \times 10^{-12}$			mol/kg	Millero et al. [1995]
RAQ11	$\text{Fe}^{3+} + 4\text{H}_2\text{O} \rightleftharpoons \text{Fe(OH)}_4^- + 4\text{H}^+$	$2.51 \times 10^{-22}$			mol/kg	Stumm and Morgan [1981]
RAQ12	$\text{Al(OH)}_3(\text{s}) + 3\text{H}^+ \rightleftharpoons \text{Al}^{3+} + 3\text{H}_2\text{O}$	$1.7 \times 10^{10}$			mol/kg	Lindsay [1979]; Bi et al. [2001]
RAQ13	$\text{Al}^{3+} + \text{SO}_4^{2-} \rightleftharpoons \text{AlSO}_4^+$	$1.0 \times 10^3$			mol/kg	Bi et al. [2001]
RAQ14	$\text{Al}^{3+} + \text{H}_2\text{O} \rightleftharpoons \text{AlOH}^{2+} + \text{H}^+$	$1.0 \times 10^{-5}$			mol/kg	Bi et al. [2001]
RAQ15	$\text{Al}^{3+} + 2\text{H}_2\text{O} \rightleftharpoons \text{Al(OH)}_2^+ + 2\text{H}^+$	$1.0 \times 10^{-10}$			mol/kg	Bi et al. [2001]
RAQ16	$\text{Al}^{3+} + 3\text{H}_2\text{O} \rightleftharpoons \text{Al(OH)}_3^0 + 3\text{H}^+$	$1.0 \times 10^{-15}$			mol/kg	Lindsay [1979]; Stumm and Morgan [1981]
RAQ17	$\text{Al}^{3+} + 4\text{H}_2\text{O} \rightleftharpoons \text{Al(OH)}_4^- + 4\text{H}^+$	$1.0 \times 10^{-23}$			mol/kg	Bi et al. [2001]

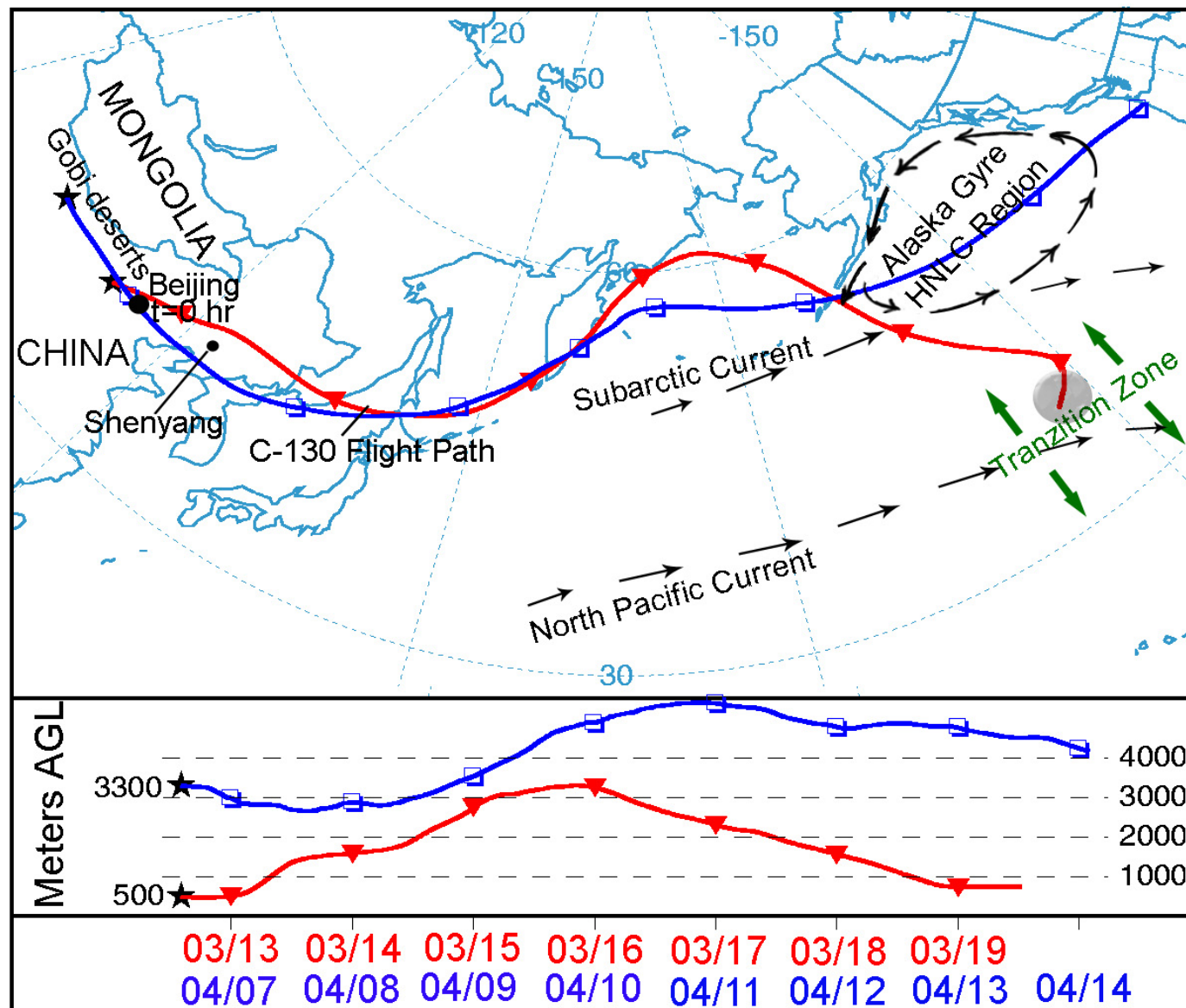
<sup>a</sup>For RAQ1, RAQ2, and RAQ3,  $K_{\text{eq}} = K^\circ \exp\left\{a\left(\frac{T_0}{T} - 1\right) + b\left(1 + \ln\left(\frac{T_0}{T}\right) - \frac{T_0}{T}\right)\right\}$ , where  $T_0 = 298.15$  K. All other  $K_{\text{eq}}$  values are assumed to be temperature-independent and are based on experimental data at 298 K.

# Two Very Different Dust Episodes



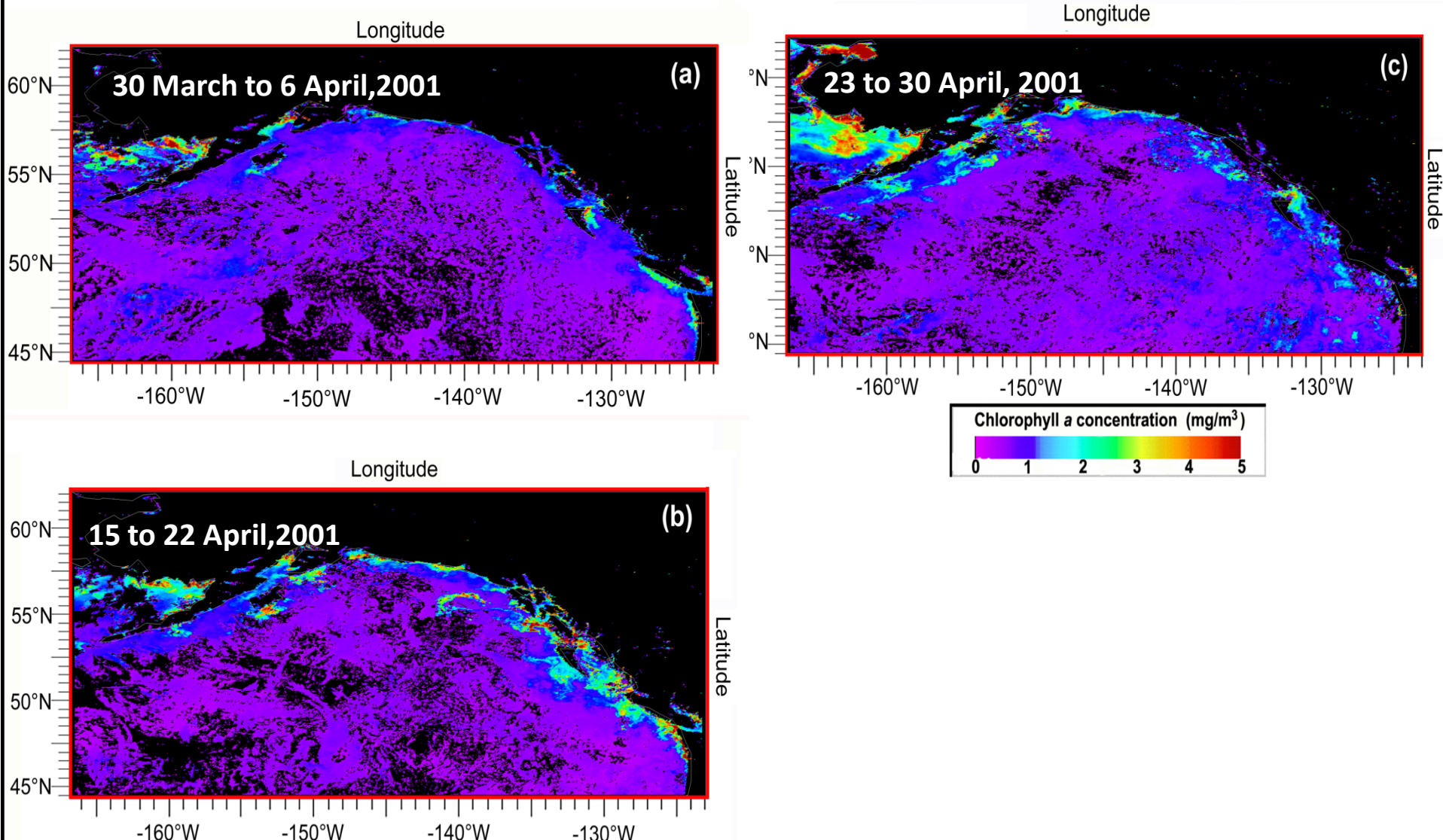
[Source: SeaWiFS Project, NASA/Goddard Space Flight Center, and ORBIMAGE]

# Trajectories Predicted by HYSPLIT for the A6 & M12



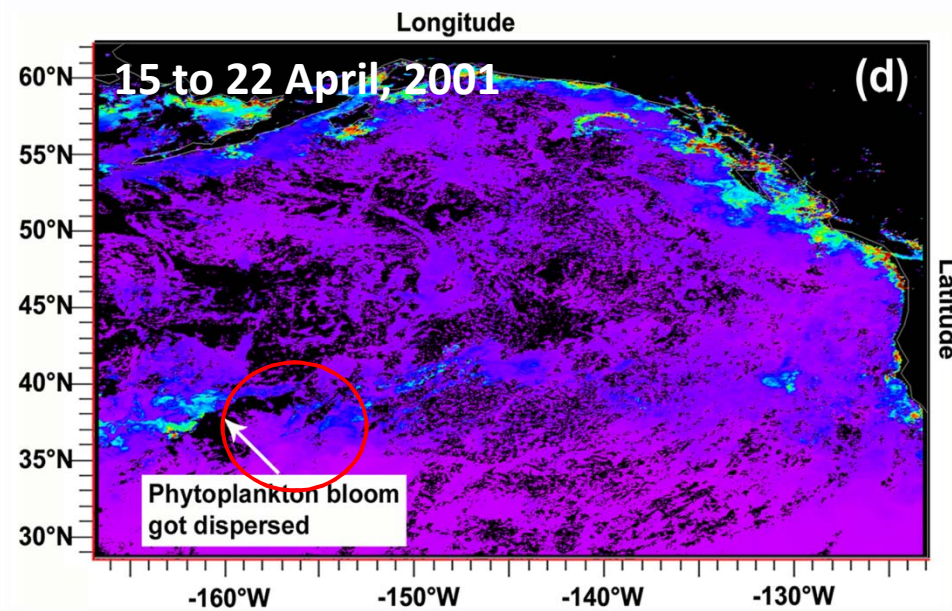
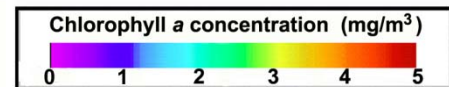
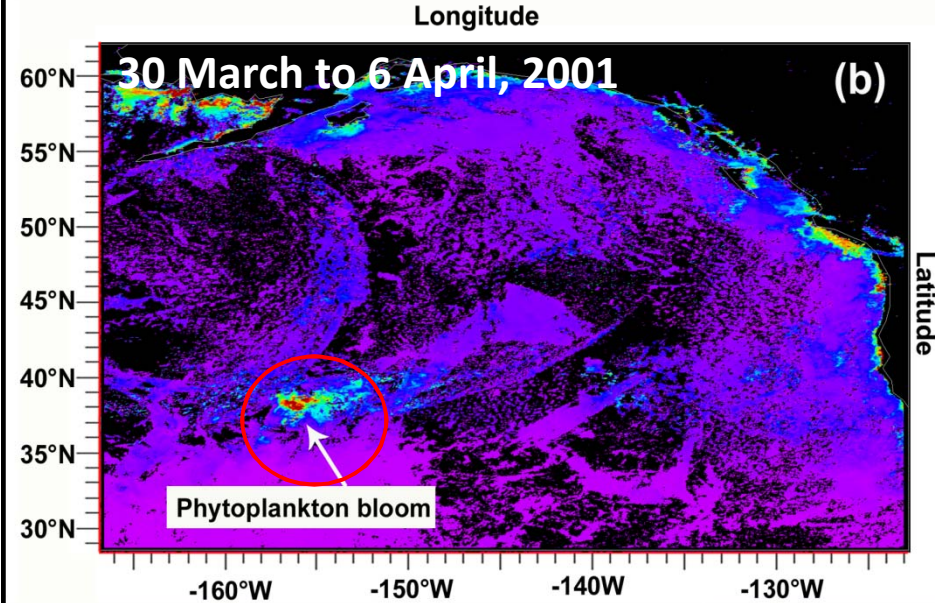
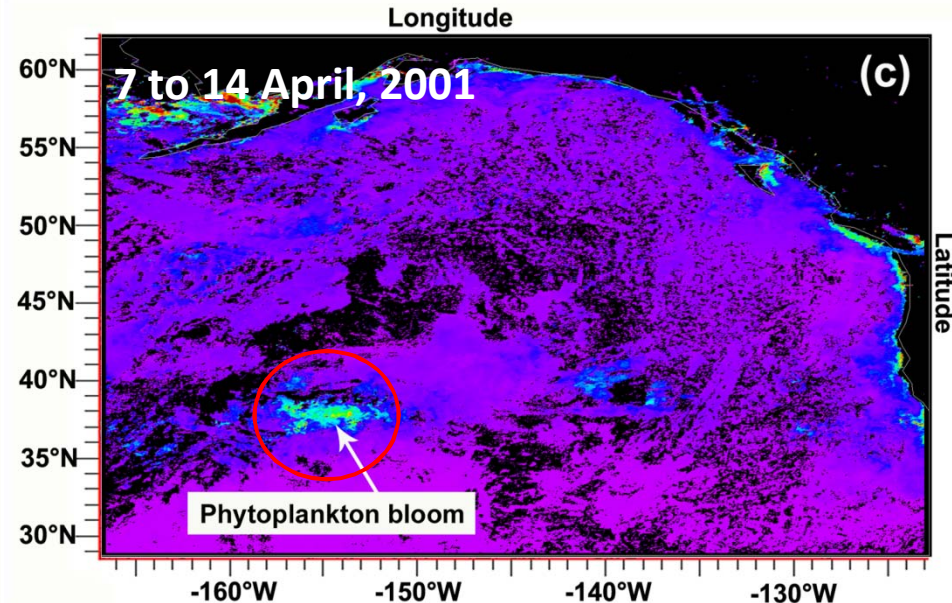
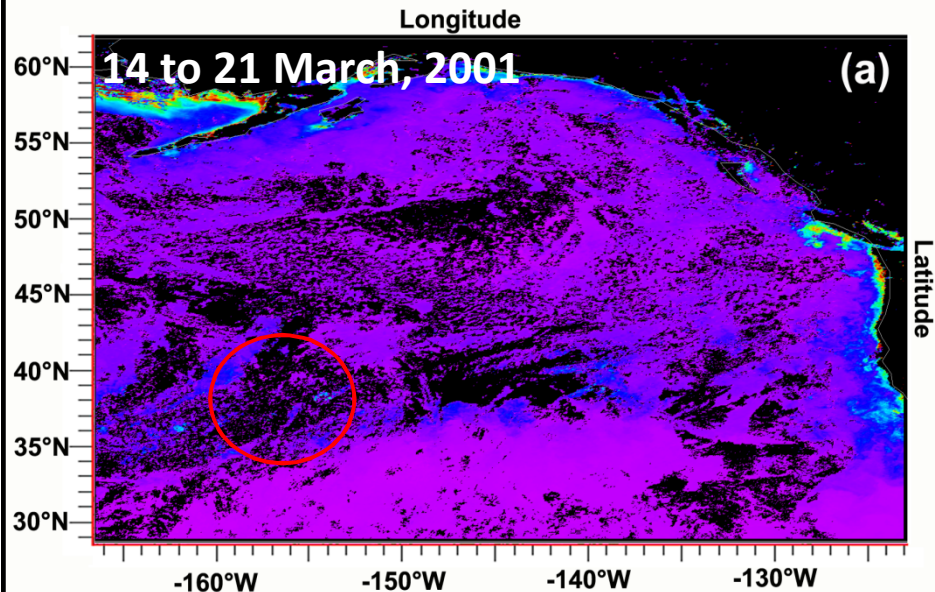
[Source: Meskhidze et al., JGR, 2005]

# MODIS [Chl-a] Over the North Pacific Ocean



[Source: Meskhidze et al., 2005, JGR]

# MODIS [Chl-a] Over the North Pacific Ocean



[Source: Meskhidze et al., 2005, JGR]

# Important Outcomes



- The relative amounts of dust and SO<sub>2</sub>
- Large dust storms – No bloom
- Unusually high amounts of pollutants
- Small dust storms - important sources of dissolved Fe, but No bloom

## Outcomes

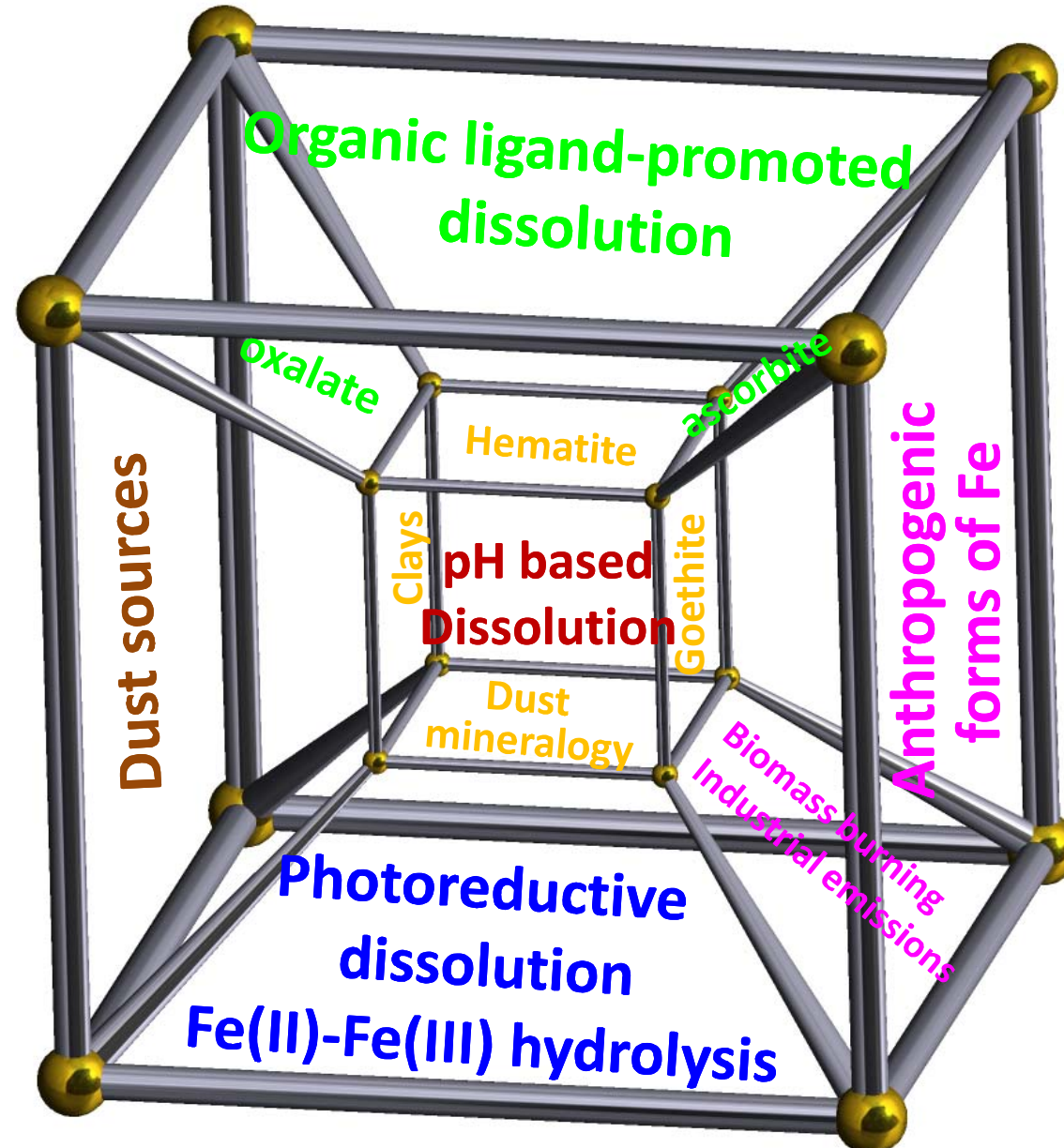
- ✓ Air pollution could enhance ocean productivity
- ✓ Air pollution controls might actually depress C-uptake in the oceans

# Overview



- 1) Introduction & motivation
- 2) Acid dissolution of iron in mineral dust aerosols
- 3) Lagrangian equilibrium model
- 4) Other mechanisms for iron dissolution
- 5) Case studies using GEOS-Chem/DFeS

# Atmospheric Fe Dissolution Scheme



# Factors Controlling Mineral Iron Dissolution During Atmospheric Transport



- Soil mineralogy at the source region
- Forms of Fe-III oxides (hematite-  $\alpha\text{-Fe}_2\text{O}_3$ , goethite-  $\alpha\text{-FeO(OH)}$ , lepidocrocite-  $\gamma\text{-FeO(OH)}$ , magnetite-  $\text{Fe}_3\text{O}_4$ , akaganeite-  $\beta\text{-FeO(OH)}$ , maghemite-  $\gamma\text{-Fe}_2\text{O}_3$ )
- Initial soluble Fe fraction (readily released Fe) 0.001 - 1.6 %
- Temperature
- Relative humidity
- Cloud cycling
- Abundance/deposition of acidic trace gases
- Photo-reductive (Oxalate) dissolution of Fe(III) oxides
- Photochemical/chemical cycling of Fe(II)-Fe(III)
- Pyrogenic (biomass burning and combustion) sources of Fe

# Fe(II) and Fe(III) Redox Cycling

## Kinetics

$\text{Fe}^{2+} + \text{H}_2\text{O}_2 \rightarrow \text{Fe}^{3+} + \text{OH}^- + \text{OH}^-$	$K_r = 76 \text{ M}^{-1} \text{ s}^{-1}$
$\text{Fe}^{2+} + \text{O}_2^- \rightarrow \text{Fe}^{3+} + \text{H}_2\text{O}_2 + 2\text{OH}^-$	$K_r = 1 \cdot 10^7 \text{ M}^{-1} \text{ s}^{-1}$
$\text{Fe}^{2+} + \text{HO}_2 \rightarrow \text{Fe}^{3+} + \text{H}_2\text{O}_2 + \text{OH}^-$	$K_r = 1.2 \cdot 10^6 \text{ M}^{-1} \text{ s}^{-1}$
$\text{Fe}(\text{OH})^{2+} + \text{O}_2^- \rightarrow \text{Fe}^{2+} + \text{OH}^-$	$K_r = 1.5 \cdot 10^8 \text{ M}^{-1} \text{ s}^{-1}$
$\text{Fe}(\text{OH})^+ + \text{OH}^- \rightarrow \text{Fe}(\text{OH})^{2+} + \text{OH}^-$	$K_r = 4.3 \cdot 10^8 \text{ M}^{-1} \text{ s}^{-1}$
$\text{Fe}^{2+} + \text{OH}^- \rightarrow \text{Fe}^{3+} + \text{OH}^-$	$K_r = 4.3 \cdot 10^8 \text{ M}^{-1} \text{ s}^{-1}$
$\text{Fe}(\text{OH})^+ + \text{H}_2\text{O}_2 \rightarrow \text{Fe}(\text{OH})^{2+} + \text{OH}^- + \text{OH}^-$	$K_r = 5.9 \cdot 10^6 \text{ M}^{-1} \text{ s}^{-1}$
$\text{HO}_2 + \text{O}_2^- \rightarrow \text{H}_2\text{O}_2 + \text{OH}^-$	$K_r = 9.7 \cdot 10^7 \text{ M}^{-1} \text{ s}^{-1}$
$2\text{HO}_2 \rightarrow \text{H}_2\text{O}_2$	$K_r = 8.3 \cdot 10^3 \text{ M}^{-1} \text{ s}^{-1}$
$\text{C}_2\text{O}_4^{2-} + \text{Fe}^{3+} \rightarrow \text{Fe}(\text{C}_2\text{O}_4)^+$	$K_r = 7.5 \cdot 10^6 \text{ M}^{-1} \text{ s}^{-1}$
$\text{C}_2\text{O}_4^{2-} + \text{Fe}(\text{C}_2\text{O}_4)^+ \rightarrow \text{Fe}(\text{C}_2\text{O}_4)_2^-$	$K_r = 4.8 \cdot 10^4 \text{ M}^{-1} \text{ s}^{-1}$
$\text{C}_2\text{O}_4^{2-} + \text{Fe}(\text{C}_2\text{O}_4)_2^- \rightarrow \text{Fe}(\text{C}_2\text{O}_4)_3^{3-}$	$K_r = 1.9 \cdot 10^4 \text{ M}^{-1} \text{ s}^{-1}$

## Photolysis

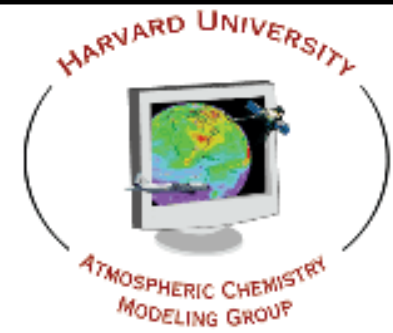
$\text{Fe}^{2+} + \text{O}_2 + h\nu \rightarrow \text{Fe}^{3+} + \text{OH}^-$	$K_p = 6.2 \cdot 10^{-4} \text{ s}^{-1}$
$\text{Fe}(\text{OH})^{2+} + h\nu \rightarrow \text{Fe}^{2+} + \text{OH}^-$	$K_p = 6.3 \cdot 10^{-4} \text{ s}^{-1}$
$\text{Fe}(\text{C}_2\text{O}_4)^+ + h\nu \rightarrow \text{Fe}^{2+} + \text{O}_2^-$	$K_p = 5.8 \cdot 10^{-2} \text{ s}^{-1}$
$\text{Fe}(\text{C}_2\text{O}_4)_2^- + h\nu \rightarrow \text{Fe}^{2+} + \text{Fe}(\text{C}_2\text{O}_4)^+ + \text{O}_2^-$	$K_p = 5.8 \cdot 10^{-2} \text{ s}^{-1}$
$\text{Fe}(\text{C}_2\text{O}_4)_3^{3-} + h\nu \rightarrow \text{Fe}^{2+} + 2\text{Fe}(\text{C}_2\text{O}_4)^+ + \text{O}_2^-$	$K_p = 5.8 \cdot 10^{-2} \text{ s}^{-1}$
$\text{Fe}(\text{C}_2\text{O}_4)^+ + h\nu \rightarrow \text{Fe}^{3+} + \text{C}_2\text{O}_4^{2-}$	$K_p = 3 \cdot 10^{-3} \text{ s}^{-1}$
$\text{Fe}(\text{C}_2\text{O}_4)_2^- + h\nu \rightarrow \text{Fe}(\text{C}_2\text{O}_4)^+ + \text{C}_2\text{O}_4^{2-}$	$K_p = 3 \cdot 10^{-3} \text{ s}^{-1}$
$\text{Fe}(\text{C}_2\text{O}_4)_3^{3-} + h\nu \rightarrow \text{Fe}(\text{C}_2\text{O}_4)_2^-$	$K_p = 3 \cdot 10^{-3} \text{ s}^{-1}$

# Overview



- 1) Introduction & motivation
- 2) Acid dissolution of iron in mineral dust aerosols
- 3) Lagrangian equilibrium model
- 4) Other mechanisms for iron dissolution
- 5) Case studies using GEOS-Chem/DFeS

# GEOS-Chem Model



## ➤ GEOS-Chem (v8-01-01) Model

### ➤ 3-D Global Chemistry Transport Model

- developed at Harvard University and other institutions around the world

### ➤ Full chemistry configuration

- SMVGEAR II chemistry solver package

### ➤ GEOS-5 meteorology

- Goddard Earth Observing System (GEOS) of the NASA Global Modeling Assimilation Office

### ➤ Detailed emission inventories

- fossil fuel, biomass burning, biofuel burning, biogenic and anthropogenic aerosol emissions

### ➤ State-of-the-art transport (TPCORE) and photolysis (FAST-J) routines

### ➤ $2^{\circ} \times 2.5^{\circ}$ grid resolution

### ➤ 47 vertical grids

## ➤ Mineral Dust and Sol-Fe Treatment

### ➤ DEAD emission scheme

- GOCART source function
- Mineral dust diameter boundaries 0.2 - 2.0, 2.0 - 3.6, 3.6 - 6.0 and 6.0 - 12.0  $\mu\text{m}$

### ➤ Seven major individual dust sources

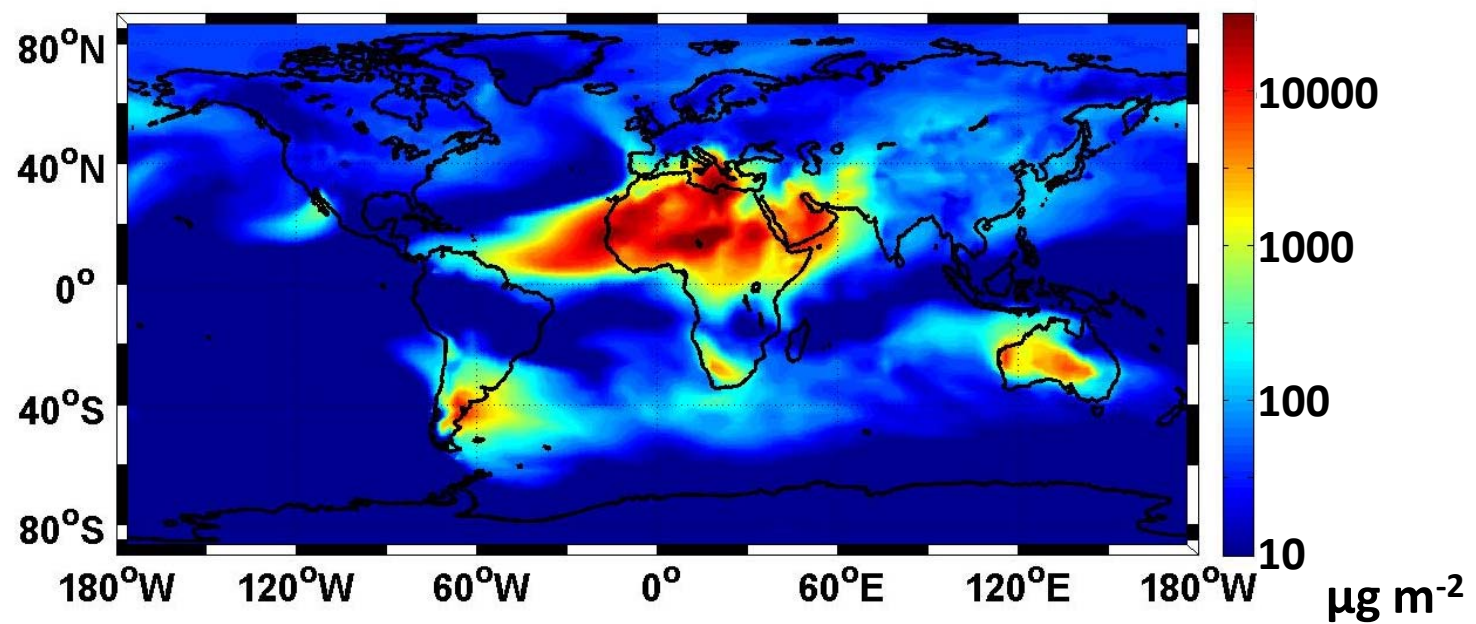
- North Africa, South Africa, North America, Asia, Australia, the Middle East, and South America

### ➤ Sol-Fe predictions

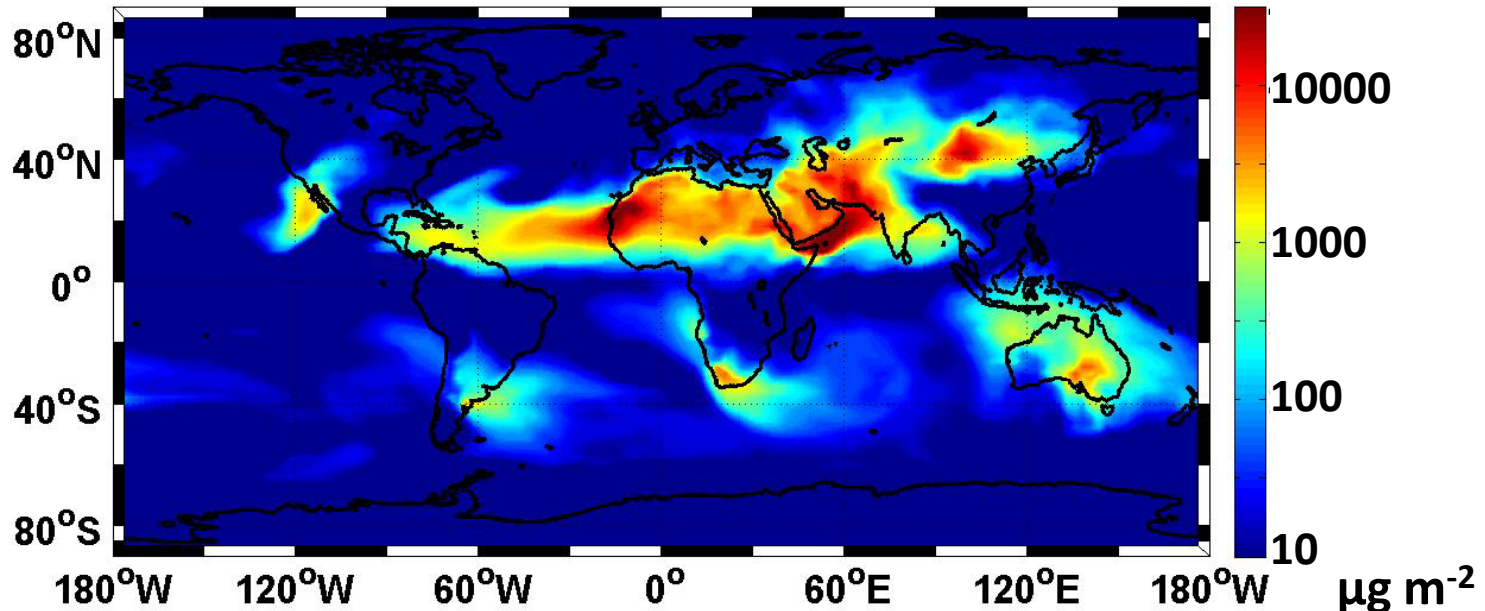
- GEOS-Chem/DFeS
- prognostic acid-based dust-Fe dissolution scheme (Meskhidze et al., 2005; Solmon et al., 2009; Johnson et al., 2010)
- organic (oxalate) promoted Fe dissolution
- Fe(II)/Fe(III) redox cycling (photochemistry)

# Mineral Dust Deposition

January 2009

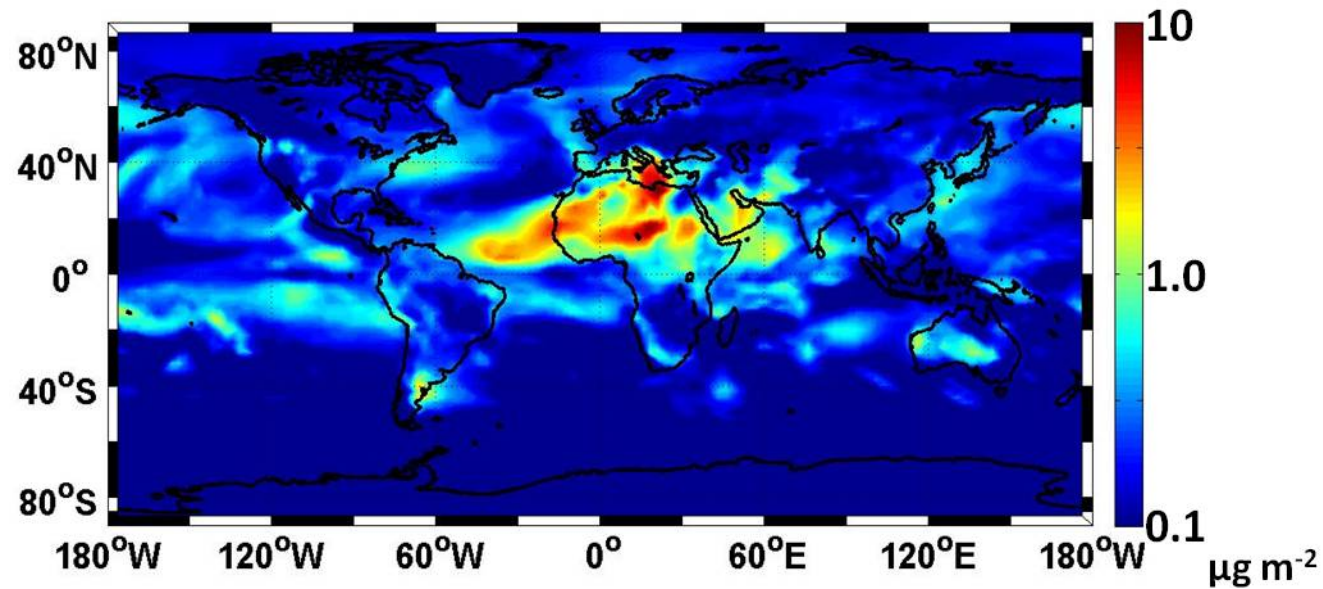


July 2009

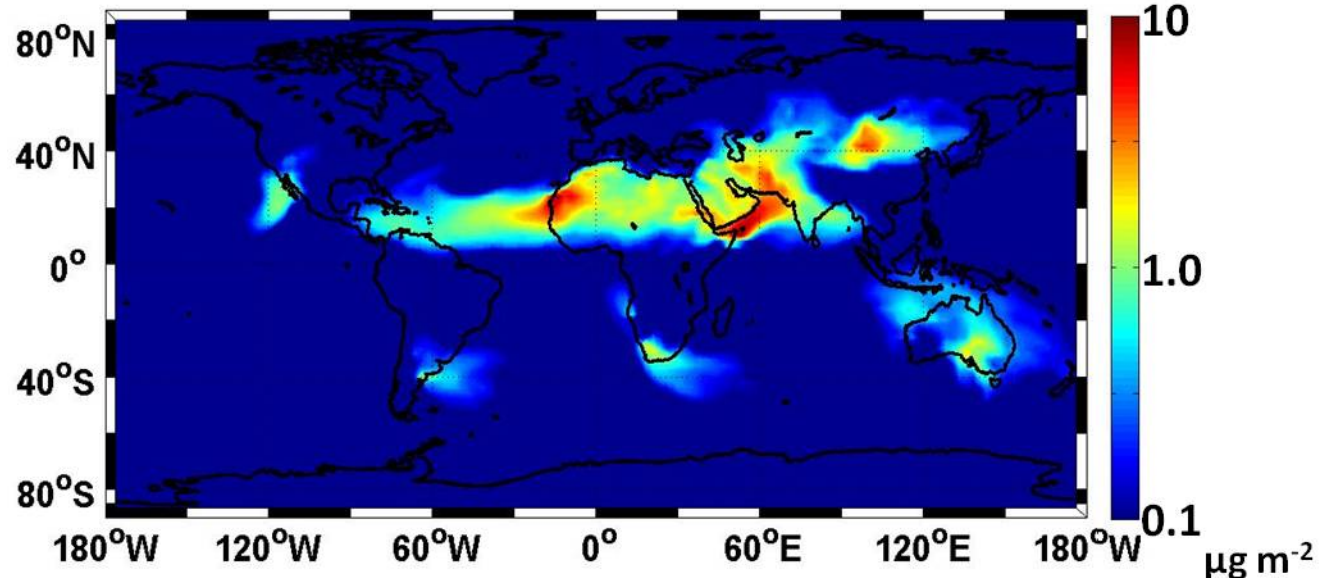


# Dissolved Iron ( $\text{Fe}_{\text{dis}}$ ) Deposition (with Organics and Photochemistry)

January 2009

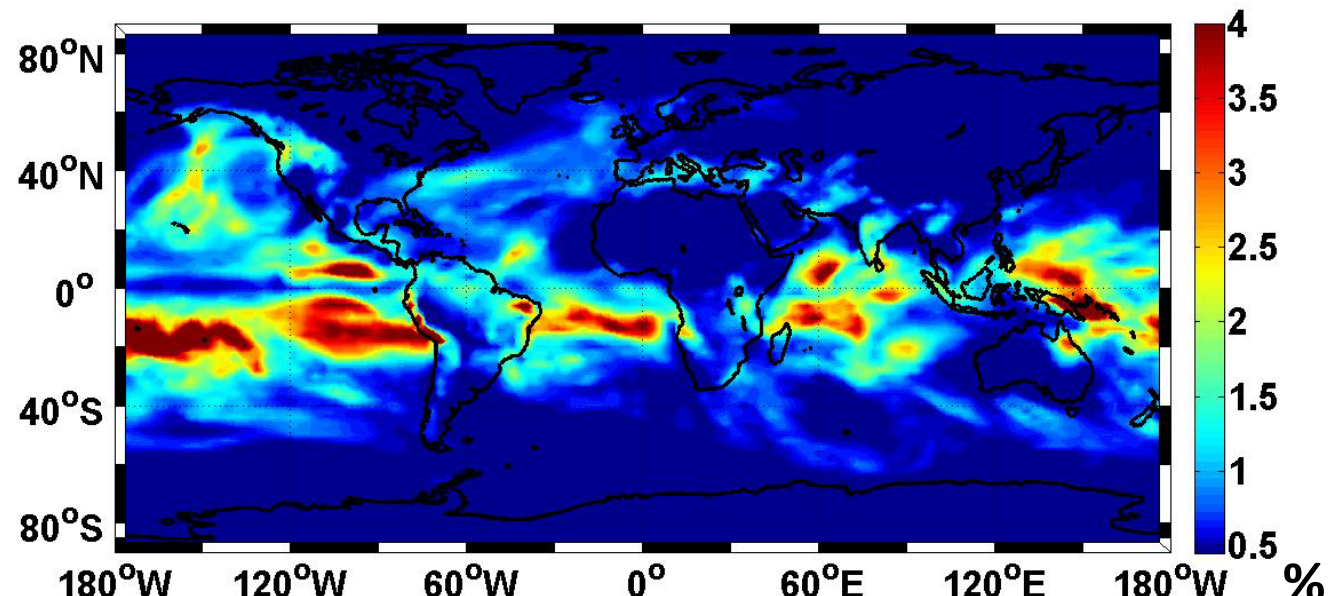


July 2009

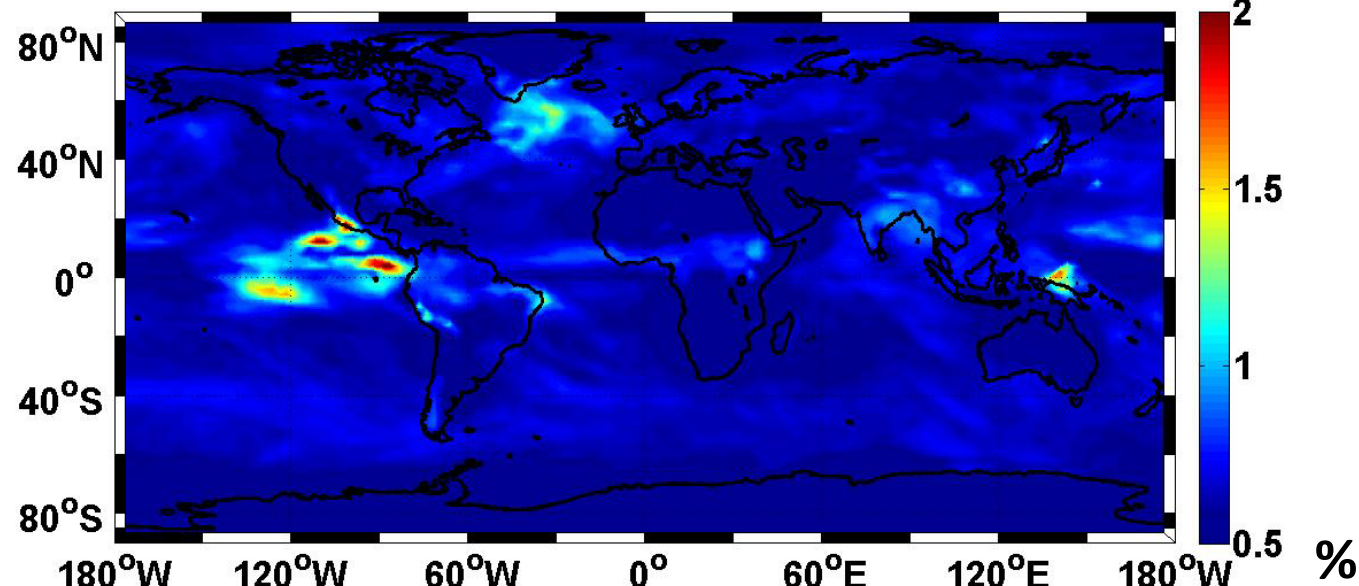


# $\text{Fe}_{\text{dis}}$ Fraction of Total Mineral-Fe (w/ Organics and Photochemistry)

January 2009

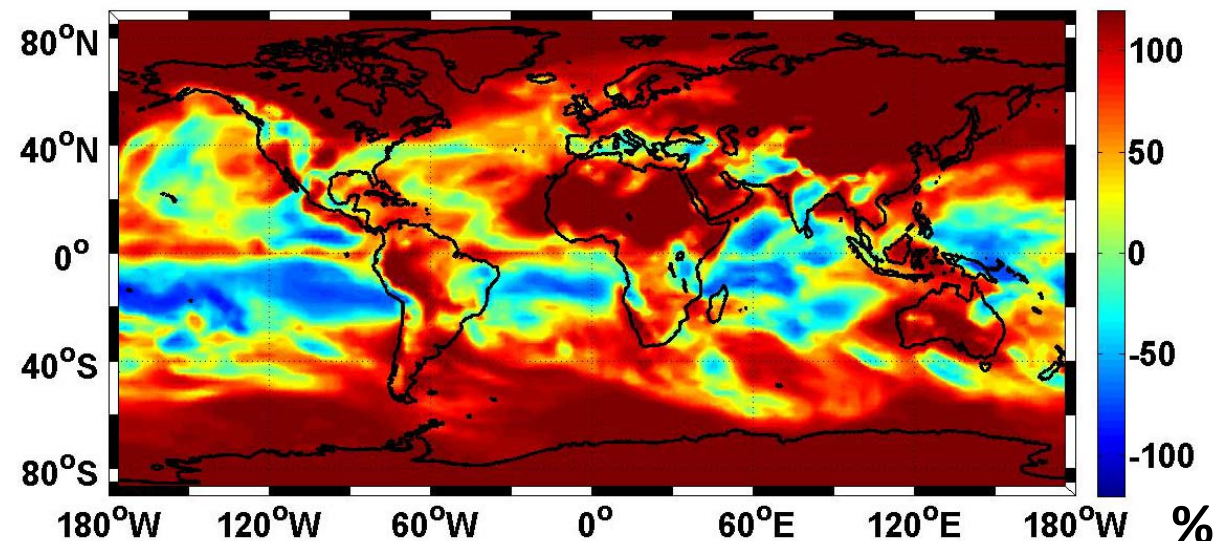


July 2009

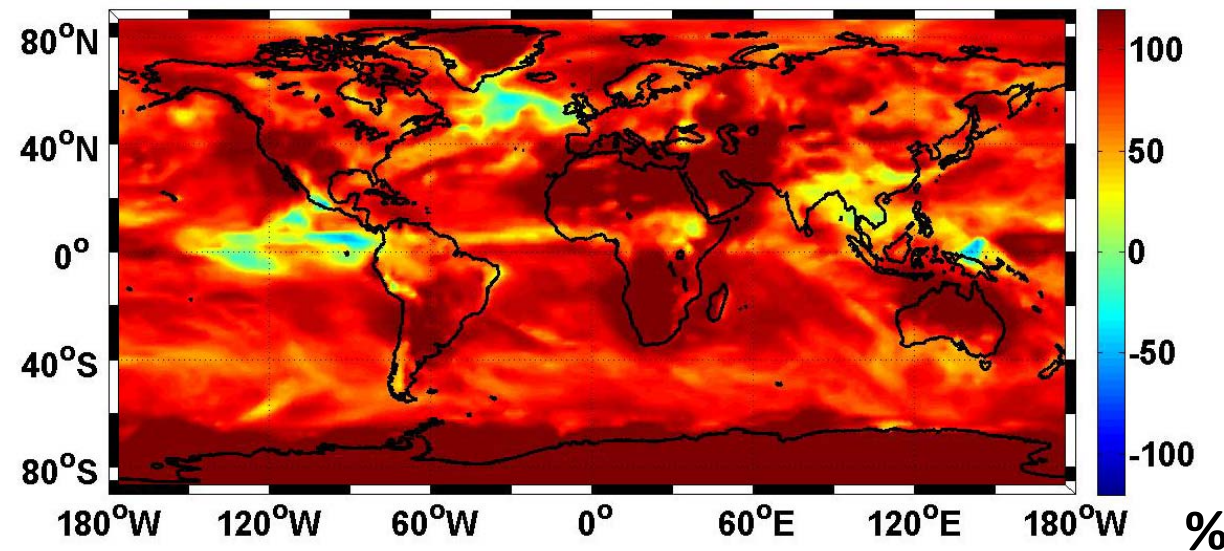


# Percent Difference in $\text{Fe}_{\text{dis}}$ Flux (1% - predicted)/1%

January 2009

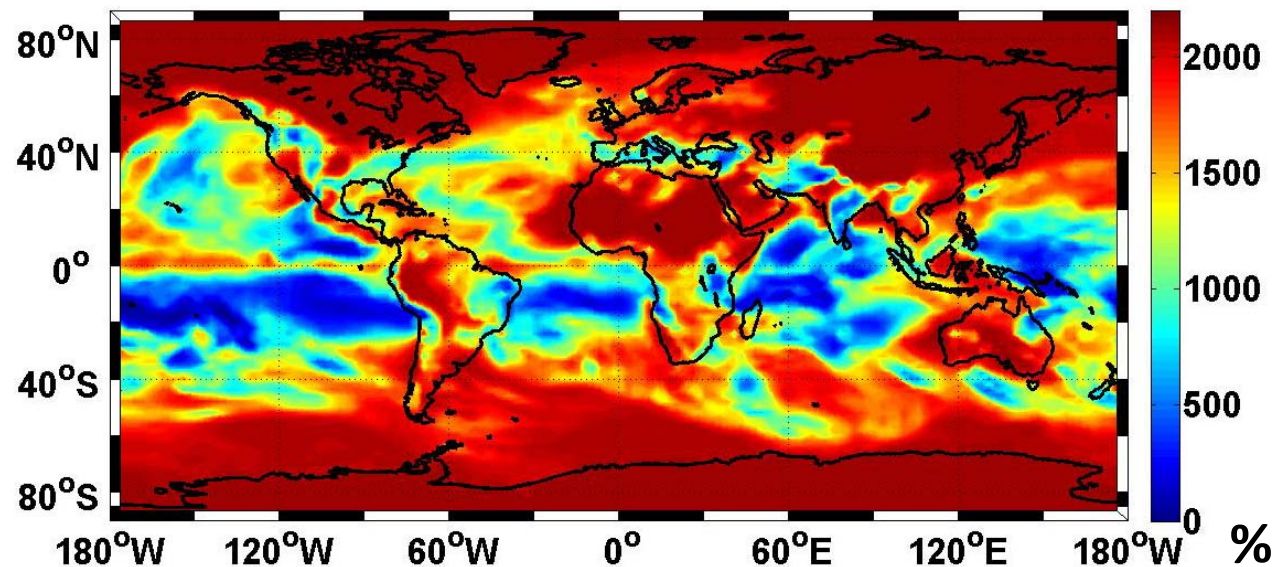


July 2009

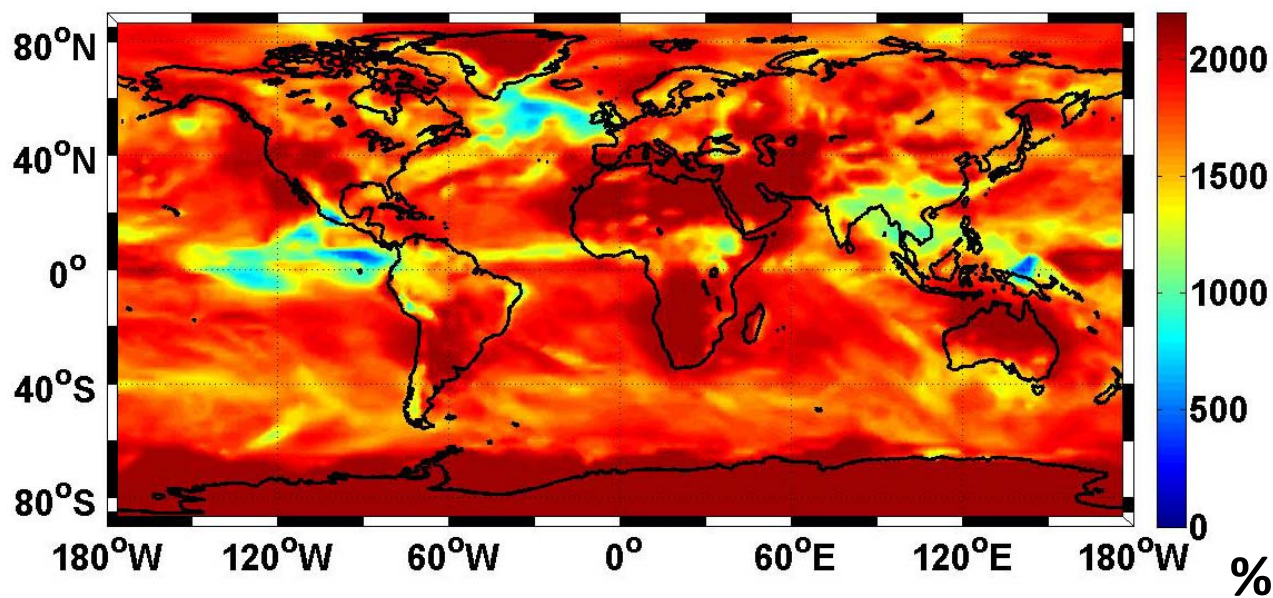


# Percent Difference in $\text{Fe}_{\text{dis}}$ Flux $(10\% - \text{predicted})/10\%$

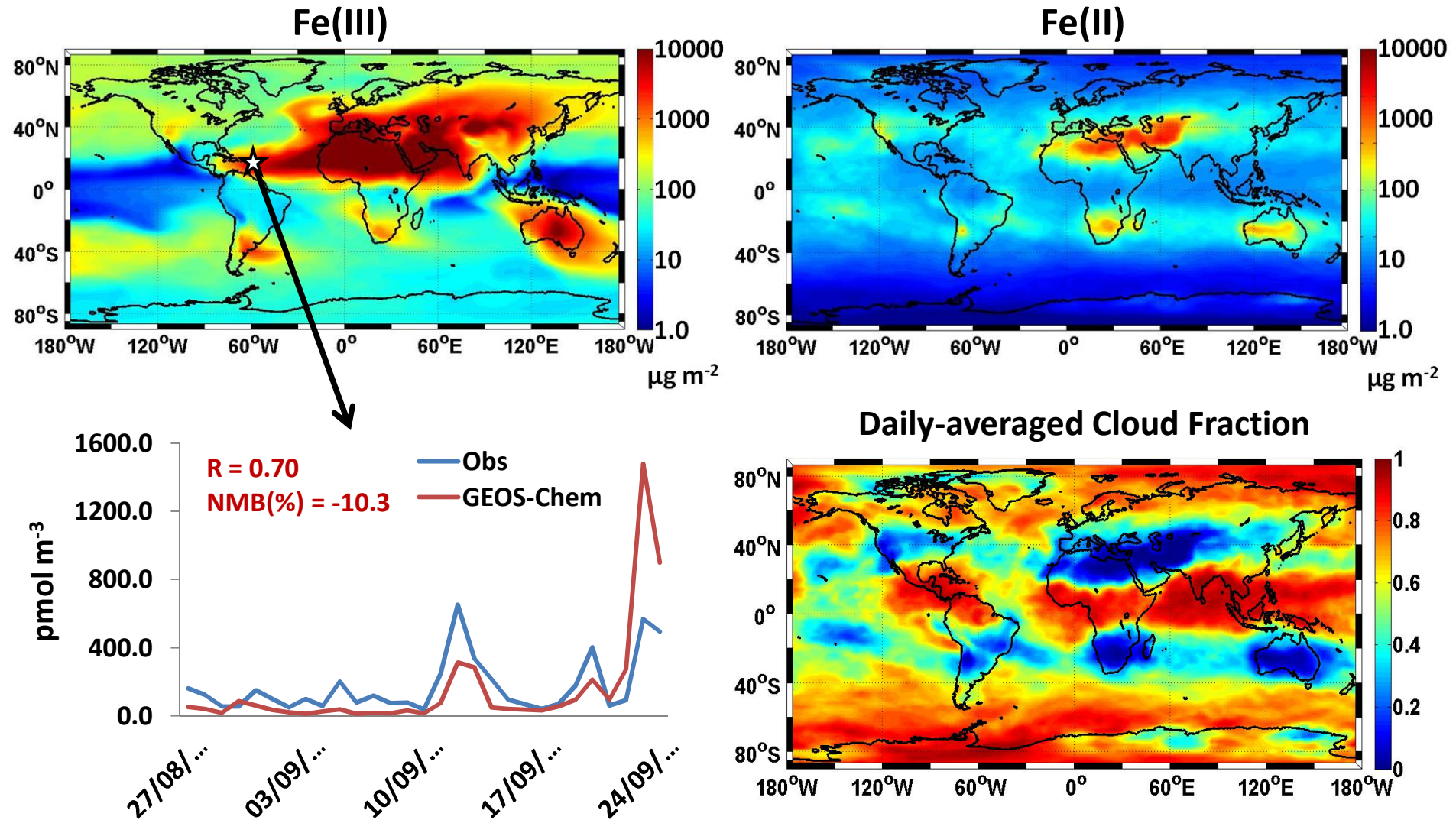
January 2009



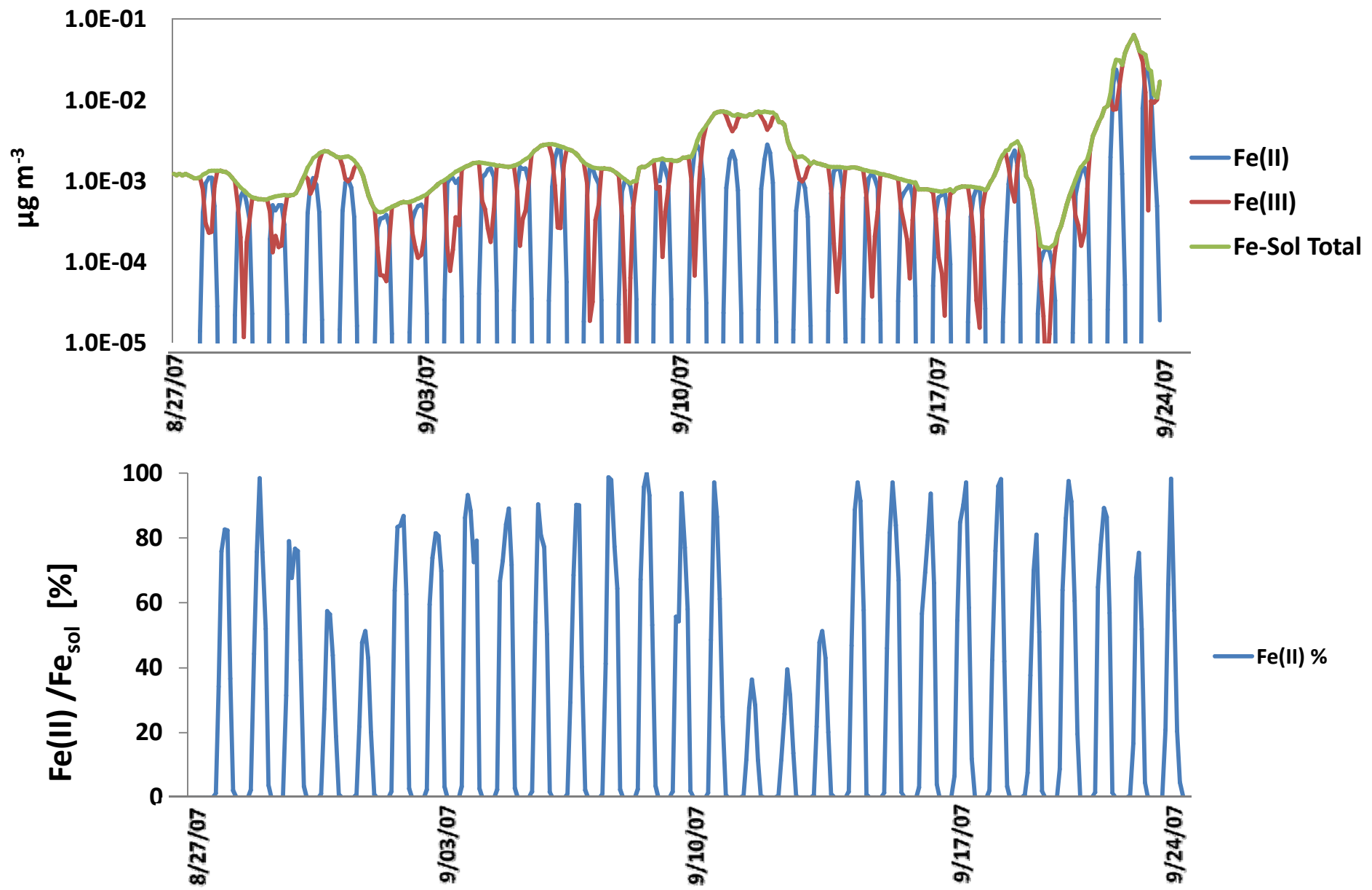
July 2009



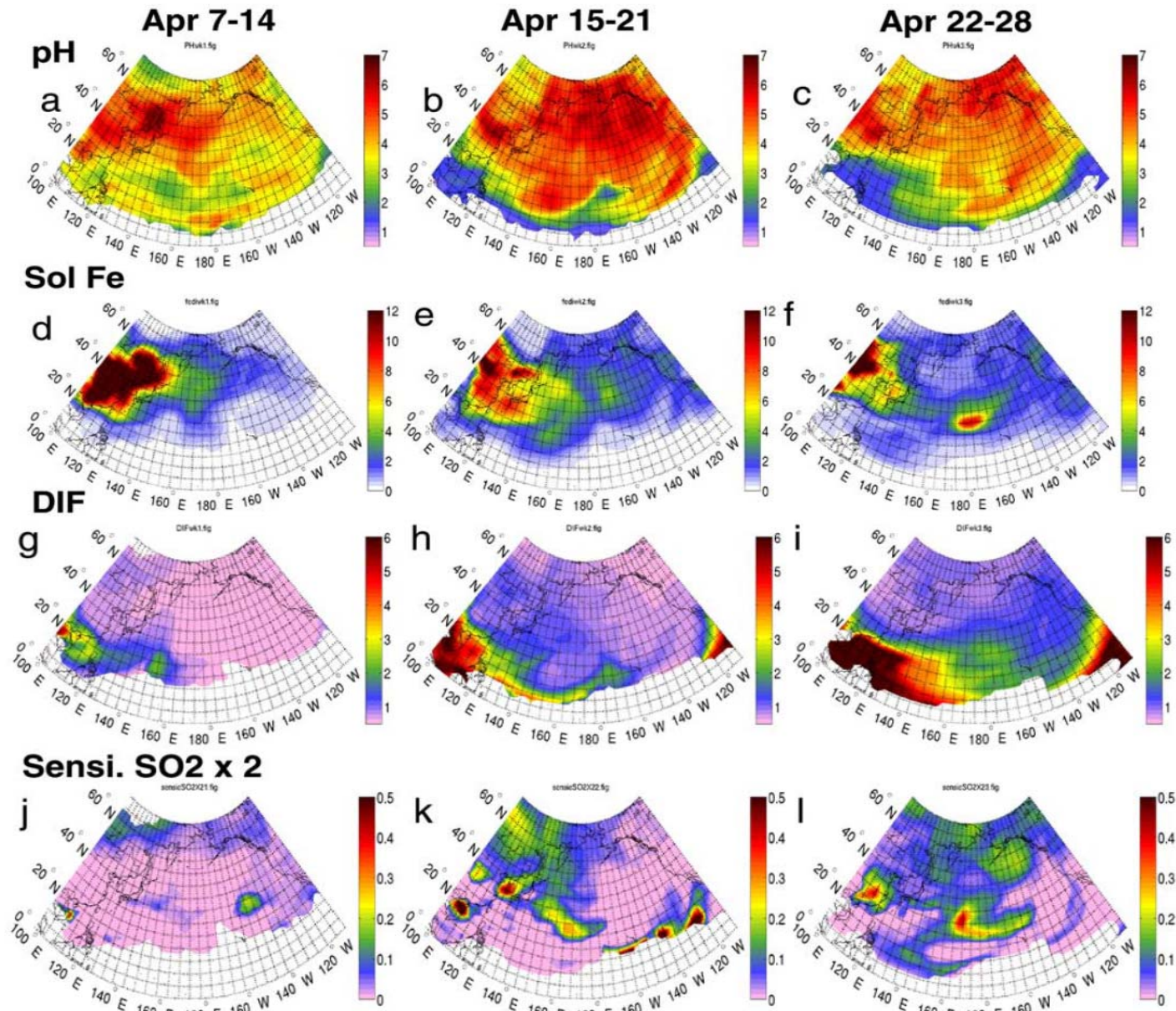
# Fe(III) and Fe(II) Daily-averaged Column Burden (Aug 27-Sep 24, 2007)



# Fe(III) and Fe(II) Time-Series

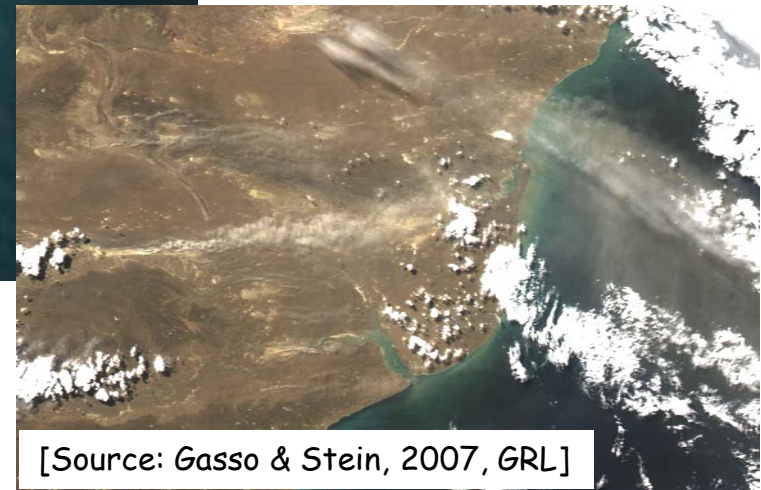
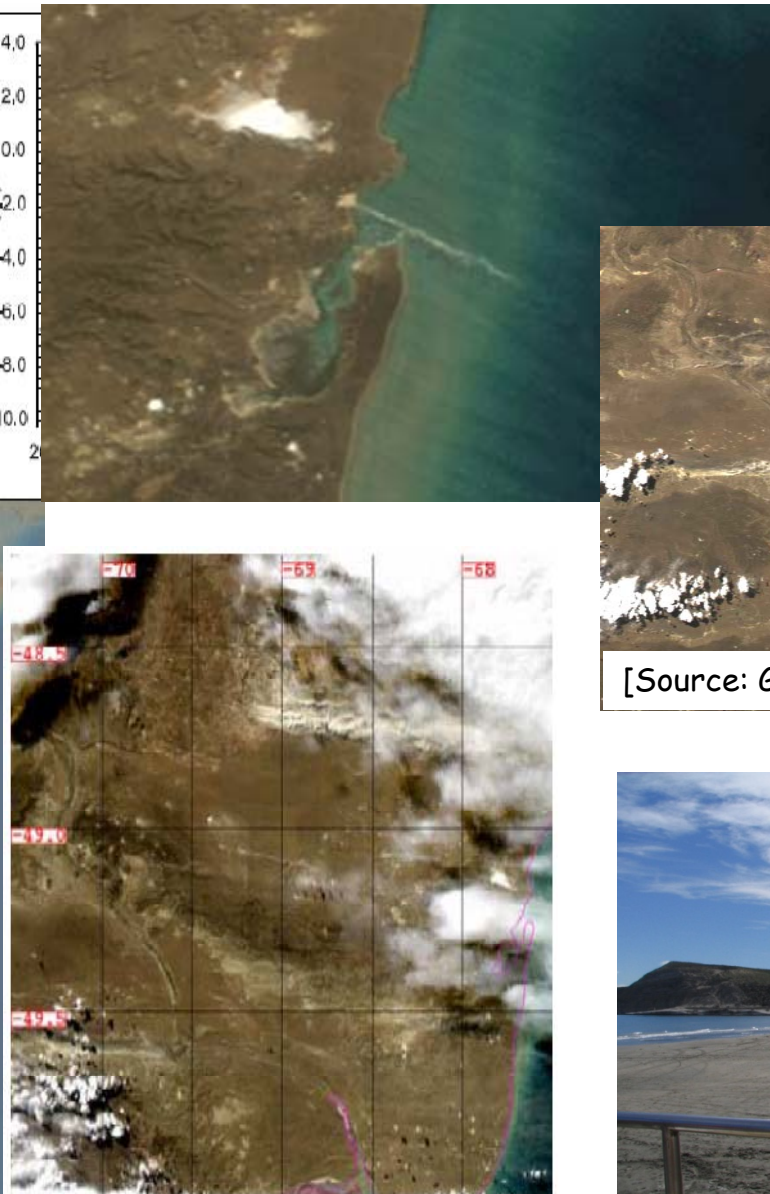
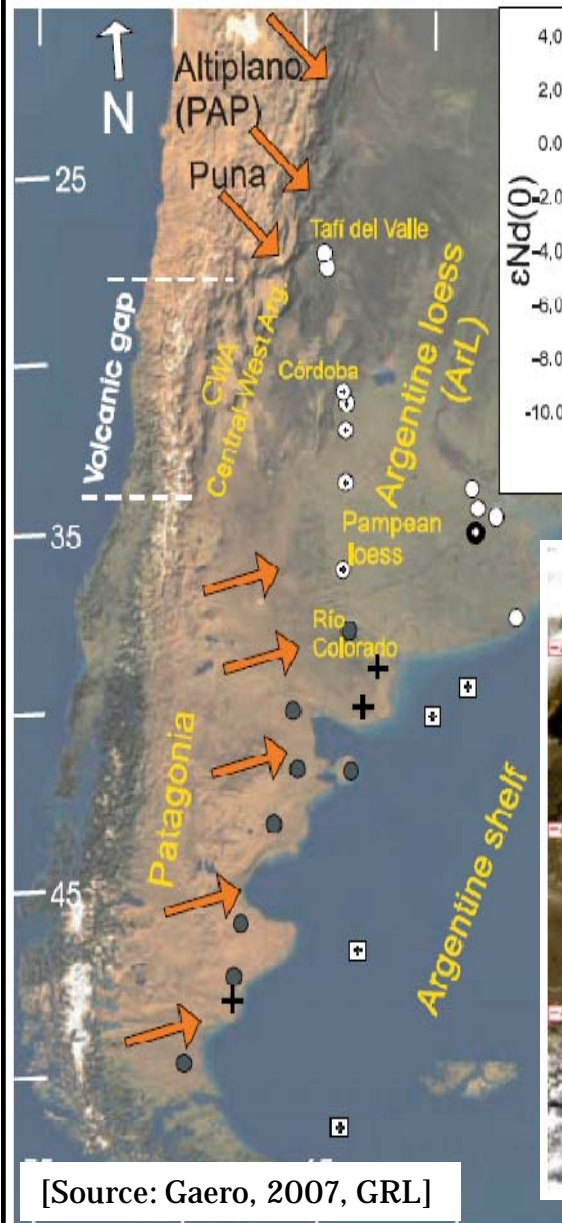


# North Pacific Ocean



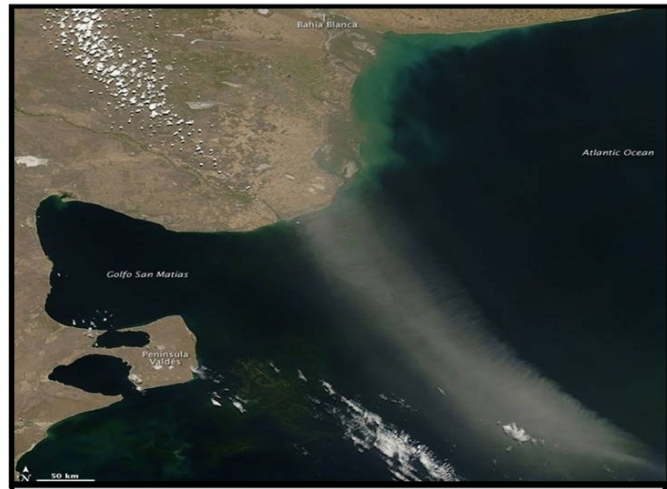
[Source: Solmon, et al. , 2009, JGR]

# Dust Sources in Patagonia



# Dust in Patagonia

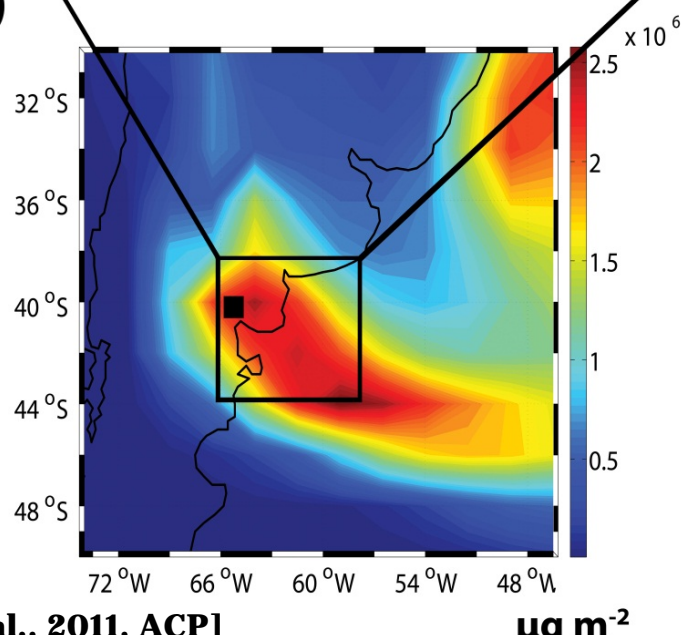
a) 23 January, 2009



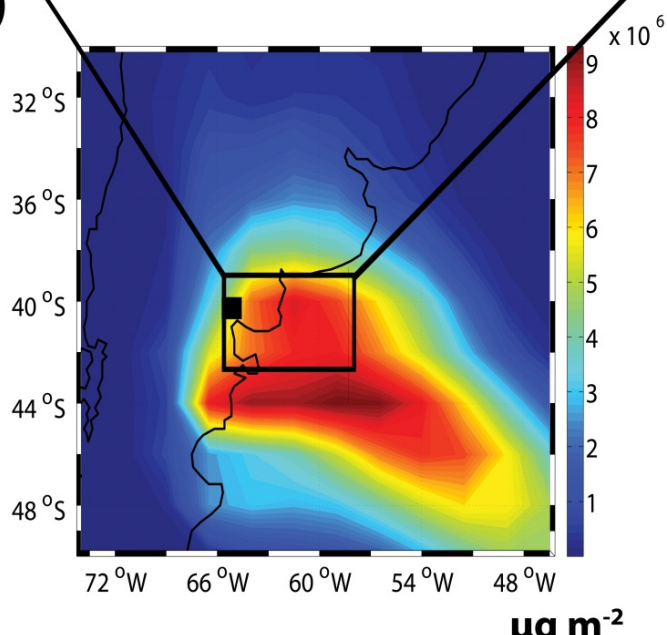
b) 17 February 2009



c)



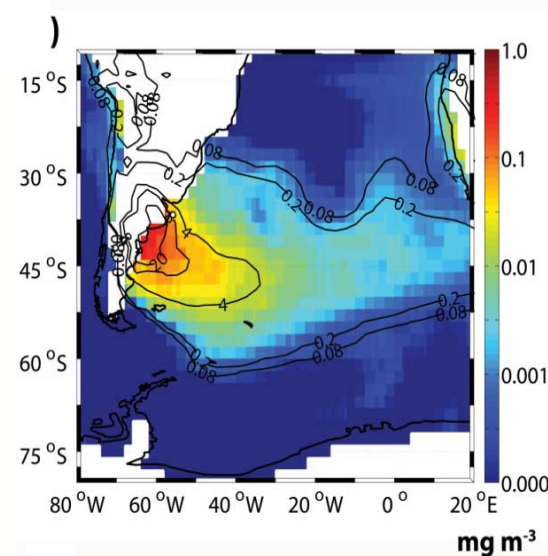
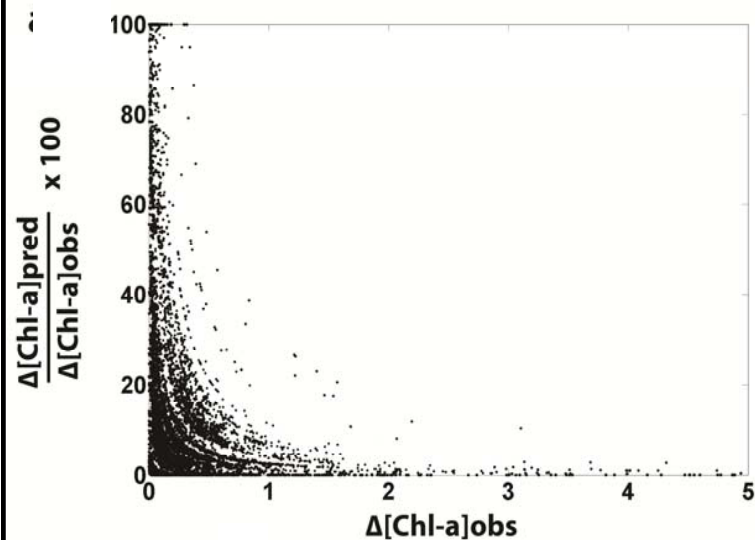
d)



[Johnson et al., 2011, ACP]

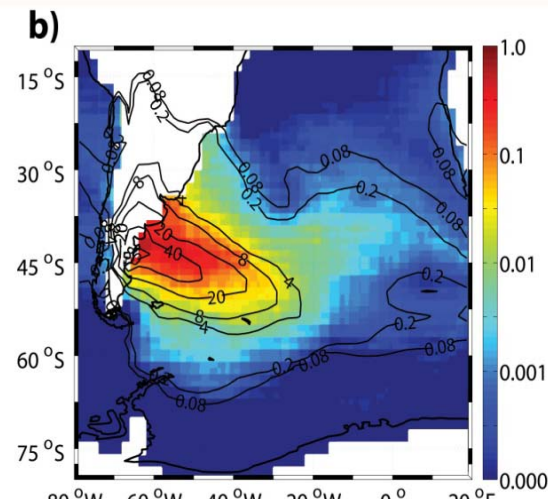
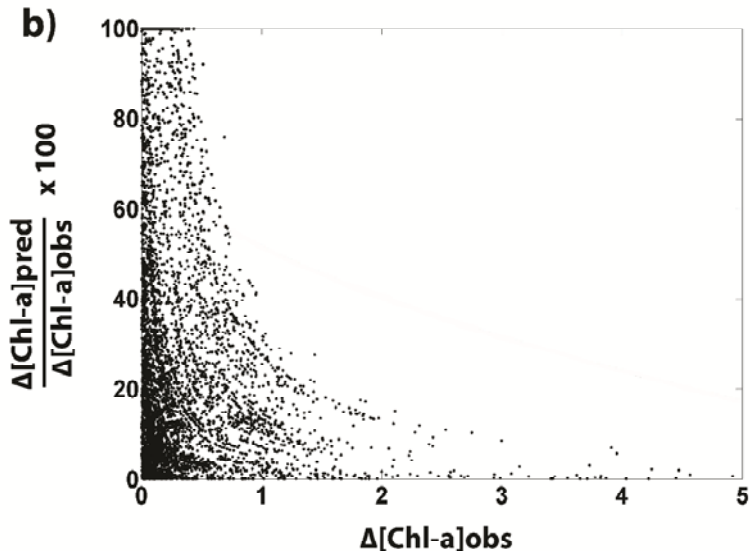
# Dust Deposition and Possible Biological Influence

23 January, 2009



- Prognostic model calculations of leachable-Fe fluxes can be used for chlorophyll production estimates
- Minimal influence in regions with remotely-sensed  $[\text{Chl-a}] > 1 \text{ mg m}^{-3}$
- Mineral dust deposition could support the background concentrations of  $[\text{Chl-a}]$

17 February 2009



mg  $\text{m}^{-3}$  [Source: Johnson et al., 2011, ACP]

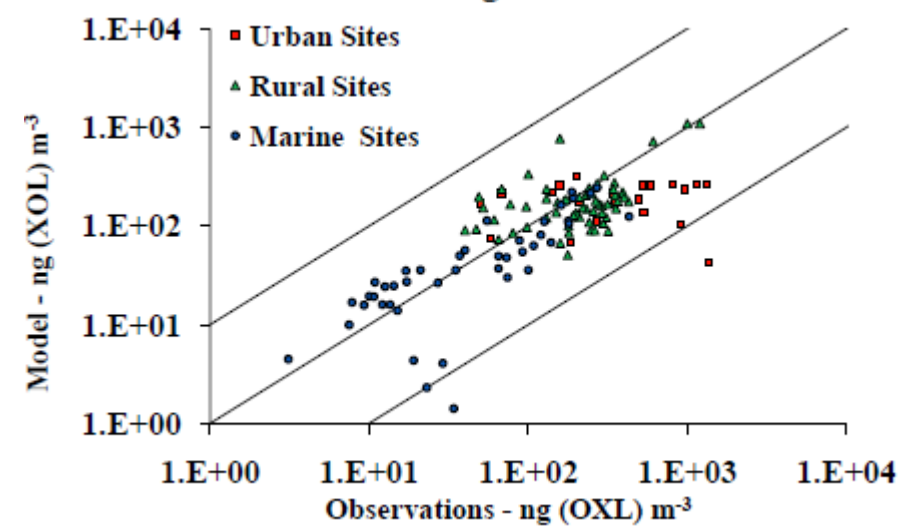
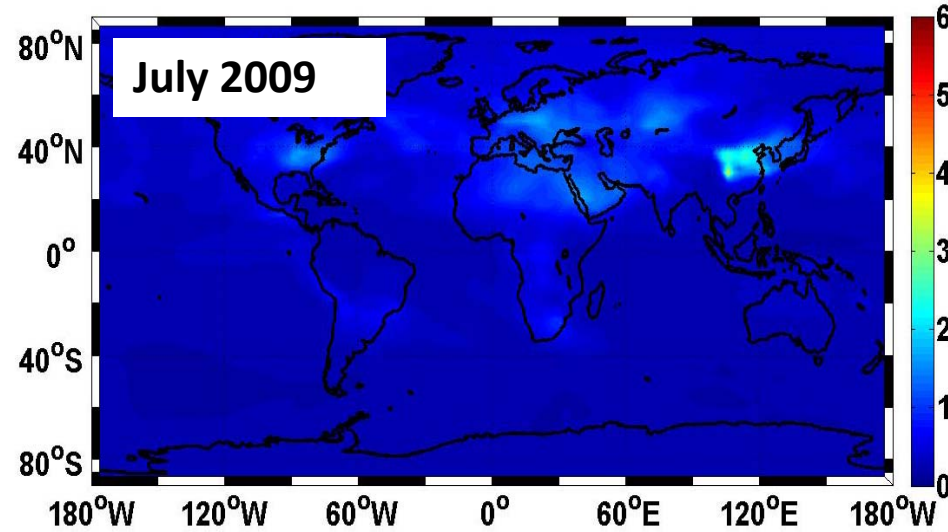
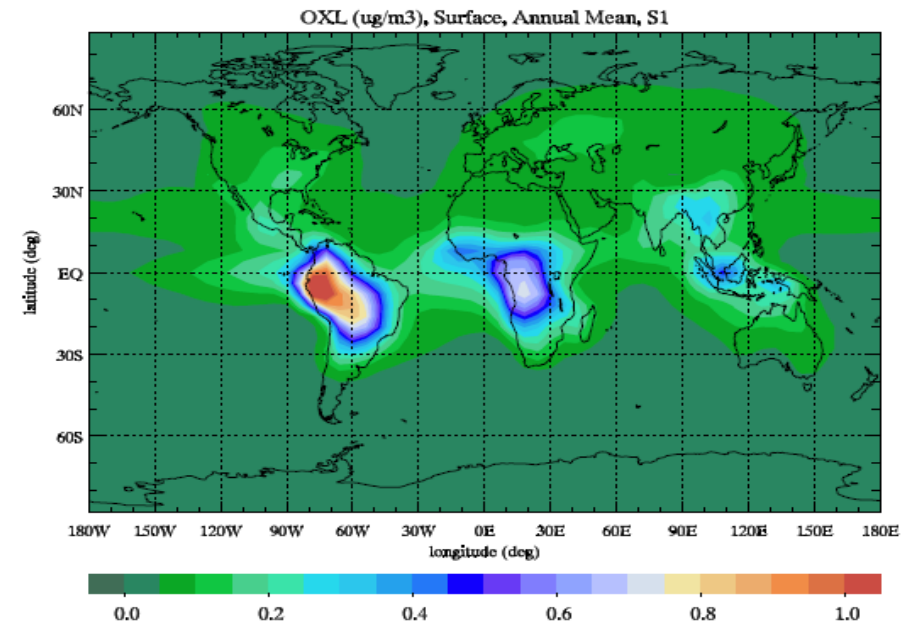
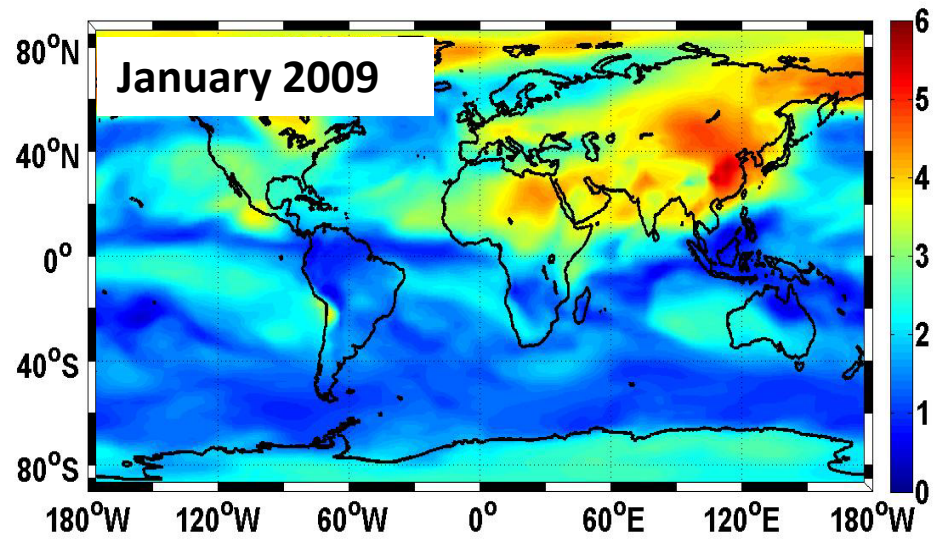
# Conclusions and Future Research



- Availability of  $\text{Fe}_{\text{sol}}$  in the oceans affects carbon cycle and climate
- GEOS-Chem/DFeS has the most comprehensive mineral-Fe dissolution mechanism currently available
- There are considerable differences between fixed percent of soluble Fe and ones calculated using prognostic dissolution-precipitation mechanisms
- More in situ sampling dust and sol-Fe is needed
- Improved remotely-sensed retrievals of [Chl-a] and aerosols are needed
- Atmospheric-chemistry transport models should be coupled with ocean biogeochemistry models to study the effect of atmospheric nutrients on carbon balance

# *Additional Slides*

# Oxalate Concentration (below 1500 m)



[Source: Myriokefalitakis et al., 2011, ACPD]